ABSTRACT

Title of dissertation:	MATHEMATICAL MODELS OF IMMUNE REGULATION AND CANCER VACCINES
	Shelby Nicole Wilson, Doctor of Philosophy, 2012
Dissertation directed by:	Professor Doron Levy Department of Mathematics Center for Scientific Computation and Mathematical Modeling

An array of powerful mathematical tools can be used to identify the key underlying components and interactions that determine the mechanics of biological systems such as the immune system and its interaction with cancer. In this dissertation, we develop mathematical models to study the dynamics of immune regulation in the context of the primary immune response and tumor growth.

Regulatory T cells play a key role in the contraction of the immune response, a phase that follows the peak response to bring cell levels back to normal. To understand how the immune response is regulated, it is imperative to study the dynamics of regulatory cells, and in particular, the conditions under which they are functionally stable.

There is conflicting biological evidence regarding the ability of regulatory cells to lose their regulatory capabilities and possibly turn into immune promoting cells. We develop dynamical models to investigate the effects of an unstable regulatory T

cell population on the immune response. These models display the usual characteristics of an immune response with the added capabilities of being able to correct for initial imbalances in T cell populations. We also observe an increased robustness of the immune response with respect to key parameters. Similar conclusions are demonstrated with regards to the effects of regulatory T cell switching on immunodominance.

TGF-beta is an immunoregulatory protein that contributes to inadequate anti-tumor immune responses in cancer patients. Recent experimental data suggests that TGF-beta inhibition alone, provides few clinical benefits, yet it can significantly amplify the anti-tumor immune response when combined with a tumor vaccine. We develop a mathematical model to gain insight into the cooperative interaction between anti-TGF-beta and vaccine treatments. Using numerical simulations and stability analysis we study the following scenarios: a control case of no treatment, anti-TGF-beta treatment, vaccine treatment, and combined anti-TGF-beta vaccine treatments. Consistent with experimental data, we show that monotherapy alone cannot successfully eradicate a tumor. Tumor eradication requires the combination of these therapeutic approaches. We also demonstrate that our model captures the observed experimental results, and hence can be potentially used in designing future experiments involving this approach to immunotherapy.

MATHEMATICAL MODELS OF IMMUNE REGULATION AND CANCER VACCINES

by

Shelby Nicole Wilson

Dissertation submitted to the Faculty of the Graduate School of the
University of Maryland, College Park in partial fulfillment
of the requirements for the degree of
Doctor of Philosophy
2012

Advisory Committee:
Professor Doron Levy, Chair
Professor Radu Balan
Professor Brian Hunt
Professor Pierre-Emmanuel Jabin
Professor John Fisher, Dean's Representative

Dedication

To Mama...

"I have devoted my entire life to increasing the number of highly qualified African Americans in mathematics and mathematics related careers. High expectations, the building of self confidence, and the creation of a nurturing environment have been essential components for the success of these students. They have fully justified my beliefs. Perhaps the most rewarding moments have come when younger faculty have undertaken the same goal and have surpassed my efforts - reaching out to the broader community to help minorities and women achieve in mathematics."

– Dr. Etta Z. Falconer, 1933 − 2002.

Acknowledgments

There are a number of people who deserve my deserve my sincerest gratitude. To all of you, I will never be able to repay the countless hours, days, and years of support you have given me.

I would first and foremost like to express sincere and heartfelt gratitude to my advisor, Doron Levy. In three short years, I have gone from a student who did not feel comfortable speaking to a professor to being a researcher who can now confidently stand by her work. The professional experience I have gained in the past few years is invaluable and would not be possible without the financial, emotional, and scientific support provided by Doron.

I also offer my sincere thanks to the other members of my committee, Radu Balan, John Fisher, Brian Hunt, and Pierre-Emmanuel Jabin for carefully reading my thesis and offering recommendations on how to improve it.

I would like to acknowledge the financial support that I have received while at the University of Maryland: the NSF BD Fellowship, teaching assistantships, and summer research assistantships. I would also like to thank the numerous travel funds that have allowed me to have the opportunity to attend conferences, workshops, and summer schools. My thanks also go to the National Science Foundation and the National Cancer Institute for funding my research assistantship in the final years of my studies.

I also owe my gratitude to the various departmental staff members who have made my life as a graduate student easier. I would like to especially thank the staff

at CSCAMM, namely Agi Alipio, Valerie Lum, and Jeff Henrikson.

I would also like to thank the following people for their positive impact on my career. Peter Wolfe taught me Numerical Analysis, but more importantly, gave me the validation that I needed as a first year graduate student. Eitan Tadmor and Konstantina Trivisa have been instrumental in providing support, encouragement and advice. Brian Hunt offered me the opportunity to be his assistant in Cameroon in Summer 2010. I am truly grateful that you and the rest of the Hands-On team allowed me to be a part of such a life changing experience. My EDGE family, in particular Silvia Bozeman, Rhonda Hughes, and Ami Radunskaya, has been absolutely instrumental in my perseverance and deserve a great deal of gratitude. And to my professors at Spelman College, the scientific foundation you afforded me pales in comparison to the principles of life you instilled in me. I am grateful to you for teaching me what it means to be a Spelman woman.

I would not have survived this graduate experience without my fellow colleagues. In particular, Cristian Tomasetti, Courtney Davis and all of my past officemates from the "Ninth Gate" and the "Zoo". Thank you to Matthew Temba and Karamatou Yacoubou Djima for taking the time to read and offer comments on this thesis. I must give a very special thanks to Amanda Galante. Most people go through the final stages of graduate school alone, but I am incredibly fortunate to have had you as my partner in crime at every step of this process. Much of my sanity over the past year can be attributed to having you to commiserate, laugh, travel and do math with.

And where would I be without my family and friends? You all are truly the

backbone that has kept me upright through this process. A special thanks to Jacinda Jack and Heather Harrington who have kept me grounded and seen me through the great and not-so-great times. To Renee, for that fateful day in front of McAlpin when the grad school decision was made, for all of the countless adventures, and for your never judgmental friendship, I thank you from the bottom of my heart. Yanne, you've given me incredible perspective while I write this "paper". Thank you for opening my eyes to the rest of the world and thank you for the adventure that is to come. To my grandparents, aunts, uncles, cousins (and kitty), your love is priceless and I thank you for always believing in me. To my little sister, not everyone can say they have a sibling who they can truly count on through thick and thin. Being your sister is an honor and a privilege. And finally, to my parents, you knew this dream was achievable long before I did. Thank you for your forethought, unconditional love, and guidance. Without you, none of this would be possible.

Table of Contents

List of Tables

List of Figures

List of Abbreviations

APC	Antigen Presenting Cell
CD	Cluster of Differentiation
CTL	Cytotoxic T Lymphocyte
CTLA-4	Cytotoxic T Lymphocyte Antigen 4
DDE	Delay Differential Equation
DNA	Deoxyribonucleic Acid
Eq.	Equation
FoxP3	Forkhead Box Protein 3
HIV	Human Immunodeficiency Virus
HPV	Human Papillomavirus
IFN-γ	Interferon-γ
IL	Interleukin
ml	milliliter
mm	millimeter
ng	nanogram
NK Cell	Natural Killer Cell
ODE	Ordinary Differential Equation
PDE	Partial Differential Equation
RHS	Right Hand Side
TC1	Transchromosomic mouse line 1
TCR	T Cell Receptor
TGF-β	Transforming Growth Factor-β
Th	Thymus derived helper T cell
Treg	Regulatory T Cell

Chapter 1

Introduction

In this dissertation we consider the dynamics of immune regulation in two contexts:

1. Determining the contribution of regulatory mechanisms to the contraction of a normal cell-mediated immune response (Chapters 2 and 3).

2. Determining the effectiveness of techniques for overcoming immunoregulatory mechanisms that are exploited by cancer (Chapter 4).

In this chapter we introduce and briefly discuss highlights from the biological background that is relevant to the present work. We also discuss general techniques that are used in addressing such biological questions with mathematical models.

1.1   An Overview of the Cellular Immune System

Adaptive immunity (in contrast to innate immunity) refers to antigen-specific defense mechanisms employed by the immune system to remove a foreign antigen. There are two major branches of the adaptive immune system; humoral and cell-mediated immunity. Humoral immunity involves the production of antibody molecules and is mediated by B-lymphocytes. Cell-mediated immunity involves the use of cytotoxic T-lymphocytes to induce apoptosis (cell death) in infected cells [79].

While much modeling and experimental work has been done on humoral immunity (e.g [3, 30, 99] or Chapter 2.1 of [73]), this dissertation focuses on mathematical models of the cell-mediated immune system.

The primary cell-mediated immune response is a process by which the human immune system responds to a foreign antigen. Upon pathogen invasion, antigen presenting cells (APCs) must migrate to the lymph nodes and present the pathogen. A naïve T cell with the corresponding specificity will then proliferate and differentiate into cells with a range of functionality. The two main classes of these T cells are helper T lymphocytes (also known as Th cells or CD4+ T cells) and cytotoxic effector T lymphocytes (also known as CTLs or CD8+ T cells). The main functionality of helper T cells is to aid in activating and directing other immune cells, while cytotoxic T cells primarily induce apoptosis in infected cells. Upon clearing the antigen, the expansion phase is followed by a contraction phase in which the immune system must retract to a resting, stable state. This process in mediated by a number of regulatory mechanisms (regulatory T cells, myeloid derived suppressor cells, IL-10, CTLA4, TGF-β, etc.). The artifacts of the preceding antigen exposure are memory T cells. These are antigen specific T cells that persist after pathogen clearance and aid in generating a more effective response to subsequent presentations of the same antigen (See Figure 1.1) [79]. What follows is a description of the key lymphocytes of the cellular immune system.
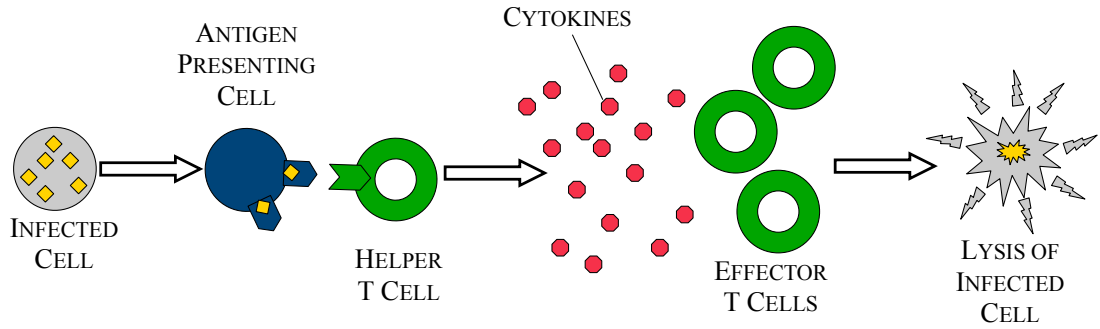
(a) A diagram showing the process by which the cellular immune system responds to a pathogen. Upon recognition of an infected cell, antigen presenting cells (APCs) will present the pathogen to helper T cells. Helper T cells will aid in activating and directing cytotoxic effector T cells to the infected cells. Cytotoxic T cells then induce apoptosis in infected cells.
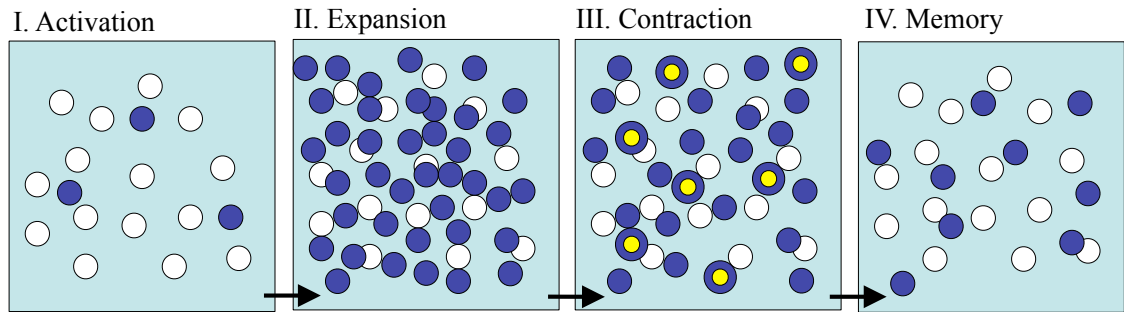
(b) A diagram showing how antigen specific T cells with a certain specificity (blue) will expand and contract into memory cells upon activation by their corresponding antigen. Cells that are blue with yellow centers stand for cells that are becoming inactive through the immune contraction process. Cells remaining in phase IV are the memory cells that persist after pathogen clearance.

Figure 1.1: Cellular immune response schematic.

Helper T Cells (CD4+ T Lymphocytes)

Helper T cells are immune cells that do not have the ability to induce apoptosis in infected cells. Instead, these cells provide essential co-stimulatory signals that are involved in the activation, proliferation and maturing processes of other components of the immune system. Upon activation by the presence of a pathogen, helper T cells proliferate by releasing a cytokine called Interleukin-2 (IL-2) which acts on helper

cells in an autocrine fashion. These activated naïve T cells will then differentiate into Th1, Th2, or Th17 cells depending on the cytokine environment. The selection of the type of helper T cell dictates the type of immune response that is elicited: IFN-γ drives Th1 cell production while IL-10 and IL-4 inhibit Th1 cell production. Conversely, IL-4 drives Th2 cell production and IFN-γ inhibits Th2 cells. Th17 cells produce IL-17 and were initially implicated in autoimmune diseases but are now thought to have their own (yet not well-characterized) effector and regulatory functions. Helper T cells are not only the driving force in the initial stages of immune expansion, but are also crucial to the contraction phase of an immune response through their relation to regulatory T cells (addressed in further detail below) [79, 96].

Regulatory T Cells (CD4+CD25+FoxP3+ T Cells)

Until recently, the discussion about the existence of regulatory T cells, has been highly contentious. Lately, concrete evidence has arisen showing that the normal immune system produces a population of T cells that are specialized for immune suppression [94]. These cells are recruited and activated during an adaptive immune response and are critical in preventing excessive immune reactions. They play a key role in the contraction phase of the immune response after invading pathogens have been successfully tackled. Along with the role they play in contracting a normal immune response, an additional function of regulatory T cells (Tregs) is to regulate immune responses that may lead to autoimmunity. Regulatory cells

4

comprise approximately 5-10% of the mature CD4+ T cell subpopulation in mice and humans. They differentiate from varying sources and are affected by a number of immunosuppressive cytokines (TGF-β and IL-10) as well as immunostimulatory cytokines (IL-2) [94, 79].

There are two types of CD4+CD25+FoxP3+ regulatory T cells. The first type, Thymus Derived Tregs, originate in the thymus and represent a distinct T cell lineage, while Antigen Induced Tregs are regulatory T cells that, depending on environmental signaling, differentiate from naïve T cells and acquire their regulatory function in the periphery. The molecular mechanism by which regulatory T cells exert their regulatory activity has not been definitively characterized and is the subject of intense research [96].

Cytotoxic T Cells (CD8+ T Lymphocytes)

Cytotoxic T cells are a sub-group of T lymphocytes that are capable of inducing death in a number of "target" cells. Targets may include:

- virus-infected cells,

- cells infected with intracellular bacterial or protozoal parasites,

- allografts such as transplanted organs,

- cancer cells.

Cytotoxic T cells express T-cell receptors (TCRs) that can recognize a specific antigenic peptide. In general, the role of CD8+ T cells is to monitor all the cells of

the body, ready to destroy any cells that express the antigen peptides that they recognize.

1.2   A Brief Overview of Cancer Biology

Cancer is the leading cause of death in the western world and is the subject of intense research, yet a widely-accepted, formal definition of the disease eludes the scientific community. In [93], Ruddon defines cancer as "an abnormal growth of cells caused by multiple changes in gene expression leading to dysregulated balance of cell proliferation and cell death and ultimately evolving into a population of cells that can invade tissues and metastasize to distant sites, causing significant morbidity and, if untreated, death of the host."

In [48], cancer biologists Hanahan and Weinberg identify six underlying capabilities that are acquired by cancer cells during tumor development. These hallmarks include the ability of cancer cells to:

1. Sustain proliferative signaling.

2. Evade growth suppressors.

3. Resist cell death.

4. Have limitless replicative potential.

5. Induce angiogenesis.

6. Invade tissue and metastasize.

Revisiting [48], in 2001, Hanahan and Weinberg extended the hallmarks of cancer to include [49]:

7. Deregulating cellular energetics.

8. Avoiding immune destruction.

9. Tumor-promoting inflammation.

10. Genome instability and mutation.

Over the past 125 years, there have been a number of important milestones in cancer research. Examples include the discovery of tumor angiogenesis, the link between environmental agents and cancer, and more recently, the genetic basis for certain cancers (for a full discussion of milestones, see [40]). In the past 10 years, there has been an increased effort towards targeted cancer therapies. These guided therapies hope to treat cancer while avoiding the toxic effects of traditional chemotherapy treatments. Molecular-targeted treatments such as trastuzumab for breast cancer and imatinib for chronic myelogenous leukemia have proved effective at targeting and killing cancer cells while causing less damage to healthy, normal cells. Other types of targeted treatments currently under investigation include cytokine therapy, anti-angiogenic therapy, and vaccination [40].

1.2.1 Tumor Immunology

The relationship between cancer and the immune system is quite complex. Burnet called the ability of the immune system to detect tumor cells and destroy

them "immune surveillance" [19]. In general, the process of immune surveillance is as follows. In the initial phases of tumor formation, the immune system is able to recognize and destroy potential tumor cells. This is followed by an "immunoediting" phase in which immune elimination is not completely successful and the tumor acquires the necessary mutations to avoid destructive immune processes. The final phase, the tumor escape phase, begins once some tumor cells have acquired the necessary mutations to avoid all immune processes and the tumor is able to grow unimpeded. It is in the tumor escape phase that a tumor becomes clinically detectable [79].

A summary of many of the mechanisms by which immune evasion occurs is provided in Table 1.1. We present a mathematical model of treatments designed to overcome some of these mechanisms in Chapter 4.

1.3   Overview of Mathematical Modeling of Biological Processes

Recent advances in scientific methods have led to a plethora of data in many biological disciplines. But, contrary to conventional thought, more data does not necessarily imply a better understanding of the topic. In mathematical biology, our general goal is to synthesize biological information by identifying the key underlying components and interactions that determine the qualitative mechanics of a biological system. To approach this goal, we make simplifying assumptions about a biological system and analyze the simplified system to glean information that may be inferred about the original biological system. This analysis involves an array of powerful

Mechanism	Description
Low immunogenicity	Some tumors do not express adhesion or co-stimulatory molecules that can be presented by APCs.
Tumor treated as self antigen	Tumors express self antigens that are not easily recognized by the immune system.
Antigenic modulation	A tumor might initially express recognizable antigens but lose them or change them as the disease progresses.
Tumor induced immune suppression	TGF-β secreted by tumor cells directly inhibits immune cells and induces activation of regulatory T cells.
Tumor induced privileged site	Tumors can create a physical barrier shielding themselves from the immune system.

Table 1.1: Mechanisms by which tumors avoid immunosurveillance.

mathematical and statistical tools.

1.3.1 Biological Scale and Mathematical Technique

Two key decisions that must be made when modeling a biological system are the physical scale at which the biological components are addressed and the mathematical modeling techniques to be used. Figure 1.2 summarizes these aspects.

In mathematical models of biological phenomena, one of the smallest scales that is typically considered is the genetic scale. There are models of gene expression, gene assembly, and gene regulation [6, 46, 72]. At the intracellular scale, mathematical models are used to study questions pertaining to signaling networks, the cell cycle, or cell decision making [39, 51, 80]. Intercellular models seek to characterize interactions between different types of cells and extracellular components. On this

9

Mathematical Technique

Statistics

Probabilistic Methods

Differential Equations & Dynamical Systems

Agent Based Modeling

Biological Scale

Genetics & Epigenetics

Intracellular

Intercellular

Tissue & Systems

Epidemiology
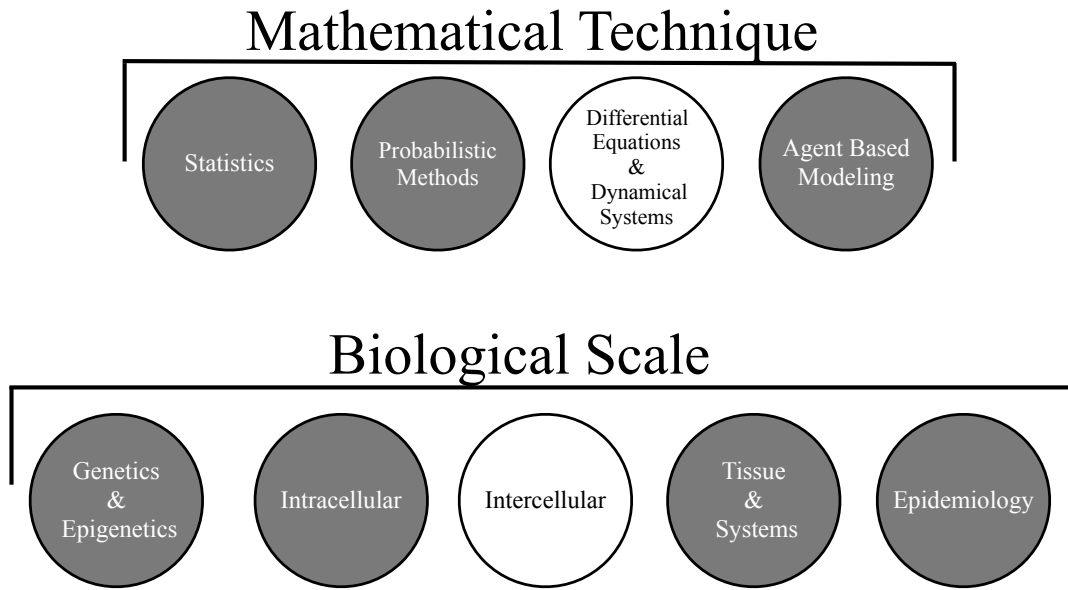
Figure 1.2: Different mathematical techniques and biological scales that are commonly used in mathematical models of biological processes. Work in this dissertation is based on differential equations as a mathematical technique and intercellular as the biological scale.

scale, a cell is considered as a single unit and models belonging to this category can be used to characterize interactions between cells of different functionality. Modeling at the tissue or epidemiological level involves large scale models of entire systems where those systems could be within organism (see [101]) or across organisms (see [35]). Recently, increases in computational capabilities have led to the development of multi scale models that seek to combine studies conducted at different scales. These mulitscale models may describe a system at many different spatial and time scales and strive to connect these scales to create a more comprehensive system (for example see [12]).

Many mathematical techniques are used to answer questions at each of these biological scales. Statistical analysis of data can give information about data and

clustering, but time dependent information is lost for many such methods. Time dependent approaches such as ordinary differential equations (ODEs), delay differential equations (DDEs), and partial differential equations (PDEs) may be used to discover dynamical information about a process. Techniques for analysis of differential equations are well developed and provide a basis for theoretical understanding. ODEs can be used in a system with homogeneous spacing where events occur on similar time scales. If spatial constraints or differing time scale constraints are a factor, PDEs are a commonly used device. DDE models are useful in cases where current conditions are dependent on conditions at a previous time. Agent based models can capture stochastic properties and emergent behavior, however due to computational complexity, these techniques are typically restricted to being used to model a small number of components.

The techniques and scale chosen in this work are highlighted in white in Figure 1.2. The questions we address in this work concern the overall time dynamics of populations of cells. Since the interactions of interest occur between cells and each cell of a specified type is assumed to have similar characteristics, we have chosen to model at the spatial level of intercellular activity. Our interest in the dynamics of these populations over time with little concern for spatial aspects, leads us to consider ODE and DDE models.

1.3.1.1 Modeling Cell Interactions

Mass action

A guiding principle of mathematical modeling that is frequently used in this work is the principle of mass action. The law of mass action is commonly used in modeling bio-chemical interactions using ODEs. This law originates from principles of enzyme-substrate reactions and states that when two or more reactants are involved in a reaction, their reaction rates are proportional to the product of their concentrations. The law of mass action relies on two assumptions:

1. The medium in which the interaction occurs must be well mixed. Under this assumption, the concentrations may depend on time but not on space.

2. The size of each species must be on the same order of magnitude. Under this assumption, the individual random probability of interactions does not need to be accounted for. Calculations using mean interaction probabilities are sufficient.

In the context of intracellular modeling, this law states that the interactions between two populations of cells occur proportionally to the number of collisions between cells from those two populations. Mathematically, if population $[ES]$ is formed through interactions between populations $[E]$ and $[S]$, then the law of mass action states that

$$\frac{d[ES]}{dt} = k[E][S],$$

where k is the kinetic coefficient of the interaction [15].

Feedback Mechanisms

A key component in determining the dynamics in intercellular systems is feedback between cell populations. The goal in modeling feedback mechanisms is to account for how the process of activation and inhibition affects dynamics within a network of cell interactions. There are three types of feedback loops that can exist between two populations of cells. These are mutual activation, activation/inhibition, and mutual inhibition, schematically shown in Figure 1.3 [50].

(a) Mutual Activation   (b) Activation-Inhibition   (c) Mutual Inhibition
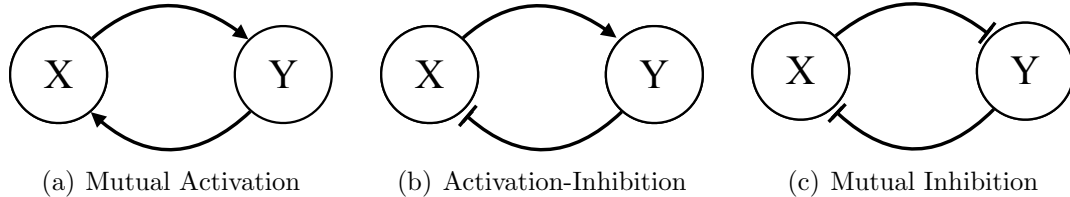
Figure 1.3: Feedback interactions between populations X and Y. (a) Positive feedback: Both populations contribute to the production of the other. (b) Negative feedback: Population X activates the production of Y which inhibits the production of X. (c) Double negative feedback: X and Y mutually inhibit each other.

In a positive feedback loop, small disturbances are amplified, increasing sensitivity to positive stimulation. Negative feedback loops can contribute to the stability and robustness of a system because this type of loop is resistant to fluctuations within the system. This type of feedback is one way to model a system designed to remain in homeostasis (equilibrium). Double negative feedback loops can be crucial in modeling cell switches and cell decision making [42, 50]. Under proper conditions, the coupling of feedback networks in differential equations determines the dynamics and stability of the system.

1.3.2 Model Parameterization

Model parameterization is an important aspect of qualifying the validity of a mathematical model. The parameters of mathematical models must be biologically relevant and physically meaningful. Parameters may be obtained from experimental data, however many model parameters are not available either because they cannot be measured using current technology, because the experiments are too expensive to conduct, or because they were never measured. Consequently, mathematical and statistical methods are commonly used to estimate unknown parameters and to determine the sensitivity of the model to those parameters. Unknown parameters can be estimated using techniques such as least squares, latin hypercube sampling or a Lineweaver-Burke plot [15, 52, 74] to name a few. Sensitivity analysis can be performed using a number of methods such as one-at-a-time sensitivity, differential sensitivity analysis, or partial rank correlation coefficients [47]. Sensitivity analysis helps to identify the key parameters that control the dynamics of the system. This can assist in validating the model with respect to current experiments/theory. It can also be used to guide experimentalists in future experimental design.

1.3.3 Computation

All computations in this work were done using Matlab Student Version 7.10.0. The Matlab function ODE23 was used for solving systems of ordinary differential equations. This algorithm uses a variable step Runge-Kutta 23 method [98]. For simulations involving delay differential equations, the Matlab function DDE23 was

used. This algorithm extends the methods of ODE23 to obtain numerical solutions of systems of delay differential equations with constant delays [98].

1.4   Overview of Dissertation

In this dissertation, we develop mathematical models to study the dynamics of immune regulation. We focus on immune regulation in the context of the primary immune response and tumor growth.

In chapters 2 and 3 we develop mathematical models of the primary immune response. We focus on two immunoregulatory mechanisms: immune contraction through adaptive regulation and functional switching of regulatory T cells. In Chapter 2, we study these immunoregulatory mechanisms in a simple ODE model. This model displays the expected expansion/contraction dynamics. A further exploration of these immunoregulatory mechanisms is done in the context of a more detailed model of the immune response in Chapter 3. We show that when compared to previous mathematical models, our model shows increased robustness with respect to key parameters. This model is also used to study the effects of regulatory T cell switching on immunodominance.

In Chapter 4, we highlight how immunotherapy might be used to overcome the effects of two regulatory agents exploited by cancer: regulatory T cells and the Transforming Growth Factor (TGF)-β protein. The goal of this study is to understand part of the complex interplay between cancer, the immune system, and the immunoregulatory mechanisms that lead to ineffective immune responses. We

develop an ODE model to gain an insight into the cooperative interaction between anti-TGF-β and vaccine treatments. This model is based on the experiments of [106]. Our model is shown to be capable of capturing the observed experimental results, and hence it can be potentially used in designing future experiments involving such an approach to immunotherapy.

Closing remarks about the work are given in Chapter 5.

Chapter 2

Functional Switching and Stability of Regulatory T Cells

2.1   Introduction

The magnitude and effectiveness of an immune response depends largely on the balance of positive and negative signals communicated by various components of the immune system. In a recent *Nature* article, Sakaguchi outlines recent biological evidence regarding the stability of regulatory T cells (Tregs) [94]. In the past, the T cell lineage has been assumed to progress downstream towards more differentiated cells. Contrary to this dogma, Tregs were recently discovered to be able to differentiate "sideways", halting their regulatory function and becoming effector T cells that secrete pro-inflammatory cytokines. Immunologists are currently working towards characterizing the conditions under which this conversion may happen. In order to understand how regulatory T cells regulate immune responses, it is imperative to investigate how they are produced and the conditions under which they are functionally stable.

While many mathematical models examine T cell lineage and differentiation [21, 43, 53, 119], here we develop a mathematical model that includes the novel consideration that regulatory T cells may lose their regulatory capabilities. Previous work has used a number of mathematical techniques in the areas of nonlinear dynamical systems and agent based modeling to investigate questions such as the

Th1 versus Th2 immune responses [43, 119] and immune cross-regulation [21, 53]. In this work, we are investigating how immune regulation arising from regulatory T cells is affected by a feedback mechanism in which helper T cells may become regulatory T cells and vice versa.

The remainder of this chapter is organized as follows: In Section 2.2.1, we review the various hypotheses concerning immune contraction and argue in favor of active suppression of immune responses by regulatory T cells. Section 2.2.2 describes the biological system highlighted by Sakaguchi and presents the experimental evidence used as a basis for our mathematical model. In Section 2.3, we present an ODE model of helper and regulatory T cell dynamics. Results characterizing the effects of Treg switching are included in Section 2.4. Closing remarks are given in Section 2.5. A further exploration of this mechanism in the context of a more detailed model of immune response will be carried out in Chapter 3.

2.2   Biological Background

2.2.1   Immune Regulation via Adaptive Regulation

The mechanisms by which the immune system contracts after an infection are debated. Razvi *et al.* demonstrated that apoptosis is the principal mediator of T cell contraction. Their experiments showed that the highest rate of apoptosis occurred at the peak of the T cell response. This led them to conclude that cells are programmed to proliferate for a fixed amount of time, after which they die [84]. An alternative point of view focuses on a division-based cell program. In this

case, cells would be programmed to divide a given number of times before dying. Renno *et al.* came to this conclusion when they studied programmed cell death in mice [87]. Yet another supported theory is that of adaptive regulation. Under this theory, during the course of an immune response, negative feedback from regulatory T cells suppress the activation of conventional T cells thereby retracting the immune response [104].

Various mathematical models have been developed in order to study the implications of the different hypotheses regarding immune contraction (see [4, 58, 116]). We review these models and make the mathematical argument for active suppression in Section 3.1.1. Here, we present the biological argument for immune contraction through Tregs.

The theory of adaptive regulation is supported by the work of Taams *et al.* who concluded that active suppression of conventional T cells by regulatory T cells is a viable possibility due to evidence that passive competition of resources (access to APCs) cannot account for the decay of the immune response [104]. It has been known for many years that regulatory T cells exist in the lymph nodes. But in 2004, Baecher-Allan demonstrated that Tregs are also present in the periphery of humans [8]. These peripheral Tregs can come from naïve T cells that have acquired a Foxp3 expression [5, 25, 68] or by trafficking from the lymph nodes to the site of inflammation using homing receptors similar to those used by other effector T cells [11, 54, 97]. It has also been shown that natural Tregs can expand clonally following antigenic stimulation and retain their suppressive function after expansion [41, 65, 117, 118]. Regulatory T cells have also been shown to suppress the proliferation

and differentiation of naïve T cells. They can also suppress the activities of mature helper T cells, mature cytotoxic T cells, natural killer cells, B cells, macrophages, and dendritic cells [78, 100, 105, 110].

The experimental evidence supports the notion that regulatory T cells exist at the site of an infection either through the homing of naturally occurring Tregs or through the induction of naïve T cells in the periphery. Similar to other T cells, Tregs activate and proliferate upon antigen specific stimulation. After expansion, they retain the ability to suppress many of the immune cells involved in the immune response. This makes a strong argument for regulatory T cells being a key mechanism of contraction of the immune response.

2.2.2   Concerning Treg Stability

A number of cytokines are essential to regulatory T cell function. These include the immunosuppressive cytokines TGF-β, Interleukin-10 (IL-10), and the immunostimulatory cytokine Interleukin-2 (IL-2). IL-2, the majority of which is derived from Th1 effector T cells, is indispensable for the maintenance of Foxp3+ Treg cells and is functionally essential for Treg development. IL-2 maintains Foxp3+ natural Tregs, triggers cell expansion at high doses, and facilitates TGF-β dependent differentiation of naïve T cells to Foxp3+ Tregs. Collectively, these factors ensure a remarkably constant number of Foxp3+ Treg cells in the immune system (about 10% of all T cells expressing the surface marker CD4), with a general increase only at sites of inflammation [96, 94].

In [94], Sakaguchi outlines experimental findings concerning the interactions between cytokine signaling, helper cell differentiation and the conditions under which regulatory T cells might convert into pro-inflammatory cells. A diagram of CD4+ T cell differentiation along with the cytokines that mediate that of differentiation are shown in Figure 2.1. Interleukins 2 and 12 drive Th1 cell production. Th1 cells are specialized at confronting intracellular pathogens. Interleukins 4 and 10 inhibit Th1 cell production while promoting the Th2 phenotype which works towards the elimination of extracellular pathogens. Th17 arise from a combination of Interleukin-6 and TGF-β signaling. These cells produce IL-17 and contribute to microbial immunity.
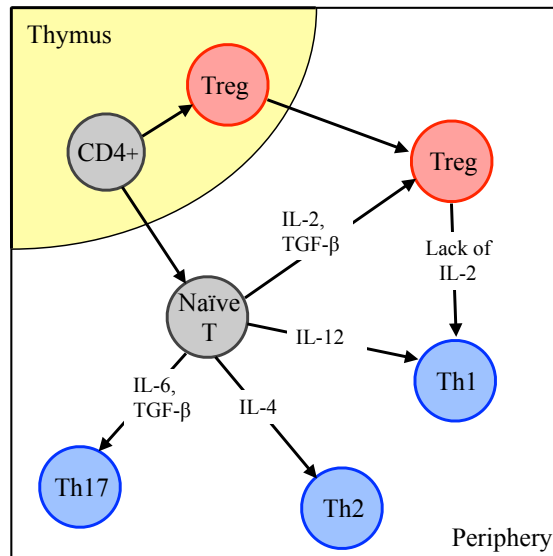
Figure 2.1: CD4+ T-cell differentiation. The thymus produces naïve T cells, which can differentiate into effector T cells, including Th1, Th2, Th17 cells, and Tregs following stimulation with antigens. In the periphery, the balances of TGF-β and IL-2 determine whether a helper T cell becomes a regulatory T cell and whether a regulatory T cell becomes a helper T cell.

Treg conversion, the process of regulatory cells halting expression of Foxp3 and

secreting pro-inflammatory cytokines, may happen only under certain conditions. The experimental evidence highlighted in [94] is as follows:

1. Regulatory T cells vary in Foxp3 expression and therefore in their susceptibility to conversion. While it is possible that all regulatory T cells are subject to conversion, it is also plausible that only a certain fraction of Foxp3+ Tregs may be plastic [120]. This could be due to variations in Foxp3 expression due to T cell lineage, maturity, genetic and environmental factors [55, 120].

2. Rubtsov et al. show that Treg cells are highly stable under certain conditions in terms of both Foxp3 expression and their suppressive function, with few cells converting into effector T cells [92]. Sakaguchi points out that this is not necessarily contradictory to previous known data and outlines ways in which this data can be consistent with other experiments.

3. When Foxp3+ Treg cells are transferred to T-cell-deficient mice, the co-transfer of T cells that do not express Foxp3 or the infusion of IL-2 prevents conversion of the Foxp3+ Treg cells to effector T cells. If Treg cells are transferred on their own to T cell deficient mice, Foxp3- T cells that have formed from Foxp3+ Treg cells will produce IL-2, which inhibits further conversion of Foxp3+ Treg cells in a negative-feedback loop [37].

2.3   Mathematical Model

We consider a simplified version of the biological system and develop a dynamical system to investigate the effects of T cell functionality switching on T cell

immunity. A schematic of the biological system is shown in Figure 2.2. We consider two cell populations: helper T cells and regulatory T cells. The helper T cell compartment combines the three types of helper T cells: Th1, Th2, and Th17 while the regulatory T cells compartment encompasses both naturally occurring and antigen induced regulatory T cells. We consider two cytokines that are primarily responsible for the facilitation of the transition between these cells. These are the pro-inflammatory cytokine, IL-2 and the pro-regulatory cytokine TGF-β.
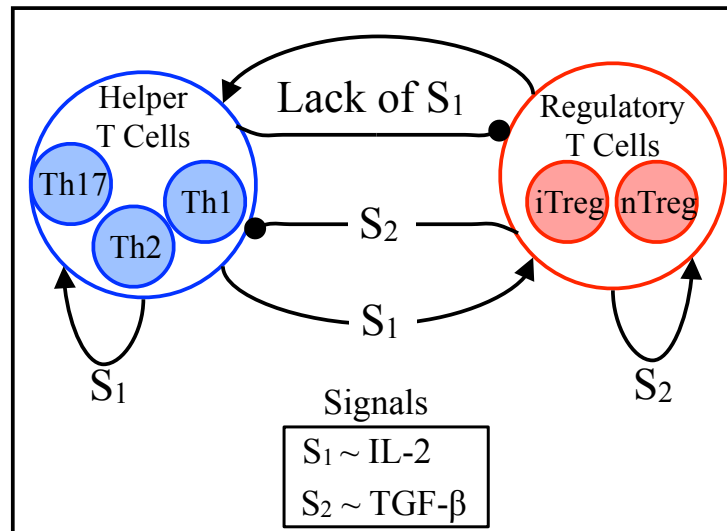
Figure 2.2: A simplified version of the biological system represented in Figure 2.1. This is the basis for our mathematical model. There are two cell populations: helper T cells and regulatory T cells. The helper T cell compartment combines the three types of helper T cells: Th1, Th2, and Th17 while the regulatory T cells compartment encompasses both naturally occurring and antigen induced regulatory T cells. Two main signaling proteins mediate this transition. They are IL-2, represented by S_1 and TGF-β, represented by S_2.

Our mathematical model is written as the following system of ODEs:

$$\frac{dH}{dt} = a(t) + \gamma \frac{S_1 H (1 - H)}{1 + cS_2} + \mu \frac{R}{1 + dS_1} - \delta_0 H - \delta_1 RH, \qquad (2.1)$$

$$\frac{dR}{dt} = a(t) + \nu S_1 S_2 R (1 - R) - \mu \frac{R}{1 + dS_1} - \delta_0 R, \qquad (2.2)$$

where,

$$S_1 = \xi H \qquad \text{and} \qquad S_2 = \beta R.$$

In this model, we follow the dynamics of helper T cells, denoted $H(t)$; and regulatory T cells, denoted $R(t)$. We model the signals between these cells in a way similar to [119]. We assume that the signals S_1 and S_2 are being produced by helper and regulatory T cells, respectively. T cell recruitment and activation depend on these cytokines. S_1 represents those cytokines predominately produced by helper T cells. Therefore although S_1 should be thought of as primarily representing IL-2 levels, it could also represent a myriad of proteins including IL-4, and IFN-γ. Similarly, S_2 represents the proteins that are predominantly produced by regulatory T cells. These include TGF-β and IL-10. We consider the magnitude of these signals to be proportional to the number of cells that produce them, and hence, $S_1 = \xi H$ and $S_2 = \beta R$. The function $a(t)$ is used to simulate recruitment of cells as a result of antigen presentation. This function is a Gaussian-like function, starting from 0, stays positive for some time, and returns to 0. A precise definition of $a(t)$ is given in Section 2.4.

The dynamics of helper T cells is described by Eq. (2.1). The second term

on the RHS of (2.1), $\gamma \frac{S_1 H(1-H)}{1+cS_2}$, describes the immune recruitment and proliferation of helper T cells. These cells are modeled as proliferating following a logistic growth rate. This growth is then modified by the present signals. S_1 signals are autostimulatory for helper T cells, while S_2 signals are regulatory. The factor $\frac{\gamma S_1}{1+cS_2}$ multiplying the logistic growth of helper T cells reflects the effects these signals have on helper T cell recruitment and proliferation. The multiplicative factor S_1 accounts for the autostimulatory effects of this population and $(1+cS_2)^{-1}$ accounts for the negative effects of the regulatory signals. The second term describes the creation of helper T cells that have originated from regulatory T cells that have lost their regulatory capabilities. Pro-inflammatory S_1 signals are required for the maintenance of regulatory T cell function. Hence, this switch from a regulatory T cell to a helper T cell occurs when there is a lack of pro-inflammatory signals produced by helper T cells. The final two terms of this equation model the removal of helper T cells from the system. These cells have both a natural death rate; assumed to be the natural death rate for all effector cells, δ_0; and an adaptive death/removal rate that is proportional to the mass action interaction with regulatory T cells, δ_1.

Equation (2.2) describes the concentration of Tregs in the regulatory T cell compartment. Regulatory proliferation and recruitment depends both on autostimulatory signals from other regulatory T cells and on signals coming from immune promoting cells. These interactions are described by the second term of Equation (2.2). Regulatory T cells are modeled as proliferating at a logistic growth rate with multiplicative factors, S_1 and S_2 indicating the presence of the co-stimulatory signals needed to facilitate this proliferation. The term $-\frac{\mu R}{1+dS_1}$ is the negative of the corre-

sponding Treg switching term in Equation (2.1). Lower levels of S_1 signals creates higher rates of transition from regulatory to helper T cells while higher prevalence of S_1 helps to sustain regulatory cells and decreases the rate of transition. Regulatory T cells have a natural death rate δ_0.

2.4   Results

We begin by demonstrating that the model (2.1) – (2.2) can capture some of the key characteristics of the immune response. After validating the model, we proceed by considering the implications of Treg functional switching within the model.

We begin our study by defining the term for antigen presentation, $a(t)$. We follow [58] and define

$$
\phi(x) = \begin{cases} e^{-1/x^2} & : x \geq 0, \\ 0 & : x < 0. \end{cases}
$$

We then set

$$
a(t) = \frac{c\phi(t)\phi(b-t)}{\phi(b)^2}, \tag{2.3}
$$

where $b, c > 0$. Graphs of $a(t)$ for $b = 5, c = 4$ and $b = 10, c = 3$ are shown in Figure 2.3.

Figure 2.4 shows a simulation of (2.1)–(2.2) with $b = 5$, $c = 4$. The parameters used in this simulation are shown in Table 2.1. These parameters are chosen to

26
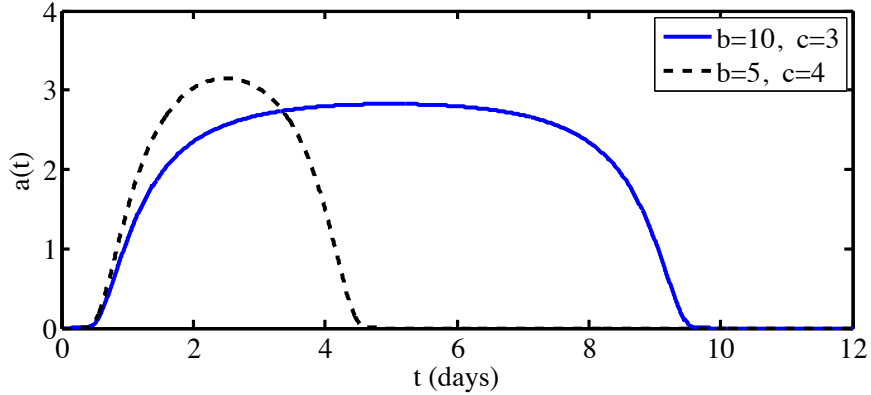
Figure 2.3: Antigen stimulation function, $a(t)$, for $b = 5, c = 4$ and $b = 10, c = 3$.

demonstrate the characteristics of the model. They are not biologically motivated. A choice of parameters that is directly tied with the biology is conducted for the more comprehensive model described in Chapter 3. The dynamics of the simulated system seem to be similar over across many values of b and c. In accordance with the antigen stimulation, we identify a growth of the helper T cells peaking soon after the peak of antigen presentation. After antigen clearance, there is a contraction of immune cells leading to a positive steady state. These lingering helper T cells correspond to the emergence of memory T cells. As a model of the cellular immune process, these results agree with the expansion, contraction, and memory dynamics seen in other mathematical models of the primary immune response [4, 58, 81]. We conclude that model, with the consideration of the new regulatory switching mechanism, displays the expected expansion/contraction dynamics.

We now study the effects of the regulatory T cell switching. What is the contribution of the $\mu \dfrac{R}{1 + kS_1}$ term to the system? Figure 2.5 shows how the magnitude of the Treg switching term changes over the course of simulation. The death rate

Parameter	Description	Estimate
γ	immune recruitment rate of helper T cells	1
c	inhibitory rate of TGF-β on helper T cell recruitment	1
μ	magnitude of regulatory T cell switching rate	9
d	magnitude of dependence of Treg switching on helper T cell signals	1
δ_0	natural death rate of effector T cells	0.01
δ_1	death rate of helper T cells as a result of interaction with Tregs	0.01
ν	immune recruitment rate of regulatory T cells	1
ξ	multiplicative factor of helper T cell signals	1
β	multiplicative factor of regulatory T cell signals	0.5

Table 2.1: Parameter values used in simulations of (2.1) – (2.2). Concentrations are measured in k/mm^3. Time is measured in days.
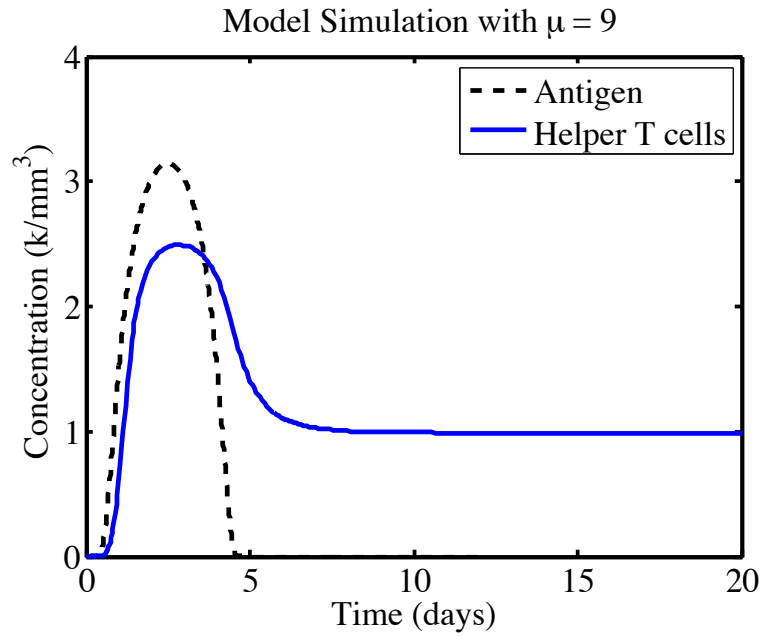
Figure 2.4: Simulation of (2.1)–(2.2) with parameters from Table 2.1. The dynamics of the helper T cells is shown in the solid line. Antigen presentation, $a(t)$, with $b = 4$, $c = 5$ is shown with a dashed line.
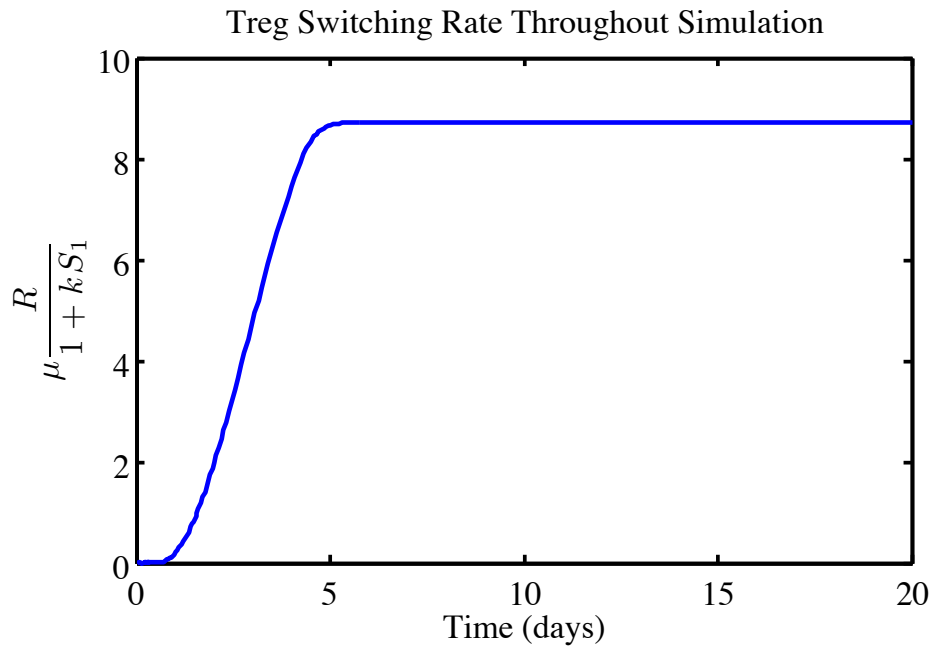
Figure 2.5: A graph of the magnitude of the transition rate of regulatory T cells due to helper T cell signals for the simulation shown in Figure 2.4.

of Tregs due to lack of signaling gradually increases as the immune response progresses. While the antigen is present, and helper T cell levels are high, the number of regulatory T cells is allowed to flourish in order to maintain control of the growing helper T cell population. Once the antigen is removed from the system (day 5 in Figure 2.5), this death rate levels out at its maximum. This new constant death rate combined with the removal of antigen stimulus serves to gradually bring the system into homeostasis. This variable death rate contributes to the dynamics in two ways. First, it allows the growth rate of the Tregs to be high enough to control the helper cells during the reaction. It allows the death rate to be high enough after the reaction to return back to normal levels of between 5 and 10 percent of the helper T cell population. Second, this mechanism allows for the presence of memory helper T cells after the reaction is over.

The velocity field of the system (with $a(t) \equiv 0$) is shown in Figure 2.6. The trajectories for different initial conditions are shown overlaid on the velocity field. The general tendencies towards the steady states can be seen. Of importance here is the ability of the system to cope with imbalances in the helper to regulatory ratio. In cases where regulatory T cells are too numerous (upper right portion of Figure 2.6, green path), there is a markedly sharp drop in the number of regulatory T cells due to the lack of pro-inflammatory signaling. When the ratio is extended too much in favor of helper T cells (right portion of Figure 2.6 and black path), we see the gradual decrease in both the regulatory T cells and helper T cell path bringing the system to an equilibrium. If imbalances occur within a normal range (e.g. if created through antigen stimulation), we see not only a decrease in regulatory T cells, but
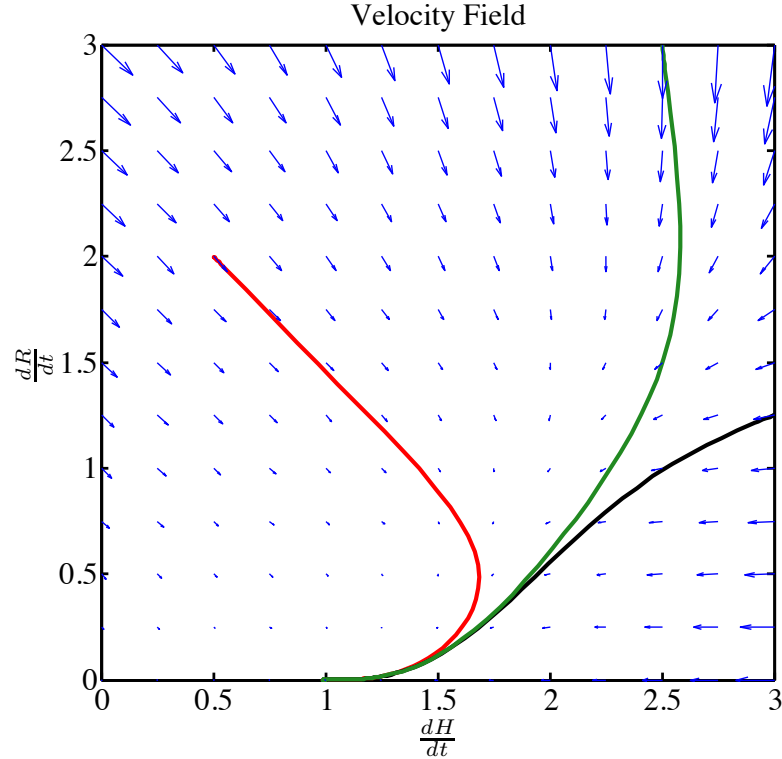
Figure 2.6: Velocity field of Equations (2.1)–(2.2) shown in blue. Trajectories over the velocity field are graphed for different initial conditions: $H = 0.5$, $R = 2$ (red); $H = 2.5$, $R = 3$ (green); $H = 3$, $R = 1.25$ (black).

also the transition of Tregs leads to an increase in the helper T cell population before decreasing back to equilibrium (black curve). This shows that even in biologically unbalanced situations, the switching mechanism allows excess regulatory T cells to contribute to the growth of helper T cells, rather than restrict it. This feedback is crucial in the stability of the system both. Biologically, this type of imbalance can occur in a number of diseases such as HIV, autoimmune diseases, cancer [18, 32, 45]. These diseases alter the constituency of immune cells and therefore mechanisms such as regulatory T cell stability may a crucial component of accurately modeling these systems.

Functional Treg switching can contribute to both the stability and the mag-
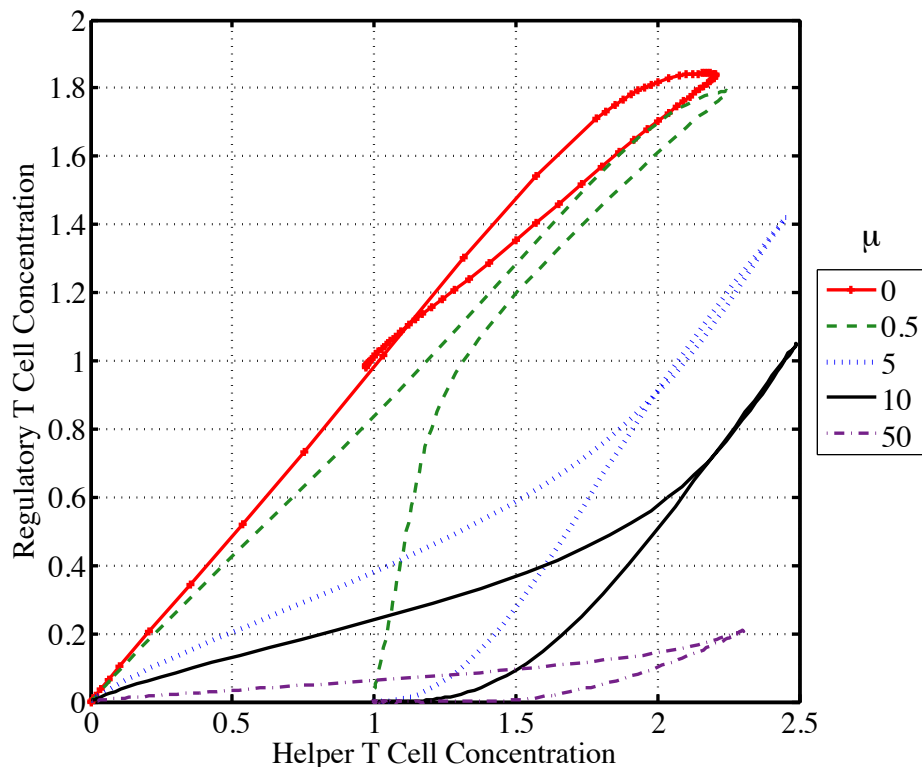
Figure 2.7: Phase portrait of helper T cells versus regulatory T cells for various values of μ.

nitude of an immune response. Because there is little to no data on the rates at which this switching occurs, we now try to qualitatively determine how the value of μ should be chosen. A phase portrait of the simulations for various values of μ is shown in Figure 2.7. The model with no regulatory switching ($\mu = 0$), is plotted in the dotted red line. For this model, as in the case with switching, the helper T cell population is able to expand and contract with respect to the regulatory T cell population. But, the final steady state of the system shows that the regulatory and helper T cell concentrations are on the same order of magnitude. While regulatory T cells have been shown to increase during an infection, it has also been shown that these cells return to their normal levels post pathogen exposure [94]. Hence we

consider the model with $\mu > 0$ to be more biologically accurate. Figure 2.7 shows that the main effect of μ is to affect the number of tregs produced in the course of an immune response. For the values of μ shown, the maximum ratio of Treg to helpers varies from 0.09 to 0.83. Biologically, we know that the concentrations of Tregs and helper T cells should not be equal, as this would contribute to disease development. This leads us to reject the smaller μ values that lead to such ratios. We also know that in the course of an immune response, the number of tregs should increase relative to their resting concentration [118]. Because these cases do not show an increase in Tregs at the infection sight, we also reject $\mu = 50$ and other high values of μ which lead to a Treg to helper T cell ratio in the range of 5-10%.

To aid in choosing an appropriate value of μ, we consider the peak helper T cell concentration produced for certain values of μ. Figure 2.8 shows a graph displaying the peak helper T cell concentration as a function of μ for μ in the range [0 20]. For these parameter values, the maximal immune response is obtained when $\mu = 9$. Consistent with what was seen in Figure 2.7, Treg switching can either contribute to the strength of an immune response or diminish it. Assuming that the natural goal of the body is to maximize the strength of the immune response, this model shows that the order of magnitude of the μ parameter should be 9. But does this imply a reasonable Treg to helper T cell ratio? For the value $\mu = 9$, the maximal ratio of Tregs to helpers is 44.9%. Though we do not have biological experiments to know what this ratio should be in the periphery, as previously discussed, it should be greater than 10% and less than 100%. This value falls in the middle of the plausible range and hence we consider $\mu = 9$ to be an acceptable choice.
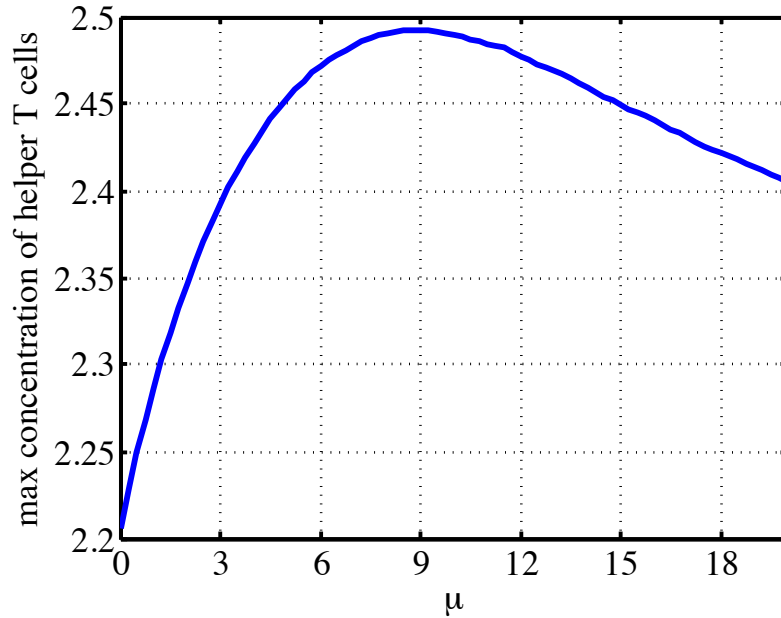
Figure 2.8: Maximum helper T cell concentration as a function of μ.

Finally, we simulate conditions that reflect the experimental setup of [37]. Here we simulate the addition regulatory T cells into an otherwise T cell deficient environment. These characteristics arise when the model is considered with initial conditions $H = 0$ and $R \neq 0$. Figure 2.9 shows the results of this simulation. As in the experiments of [37], simulations show the regulatory T cell population decreasing due to conversion to helper T cells. In finite time, a balance of signals is achieved and the populations achieve a non-zero equilibrium. This property of the model has not been seen in past models of the cellular immune system. It shows that even in the case of extreme imbalances of initial conditions, this Treg switching mechanism serves as a stabilizing mechanism and the system is able to recover to a biologically favorable state.
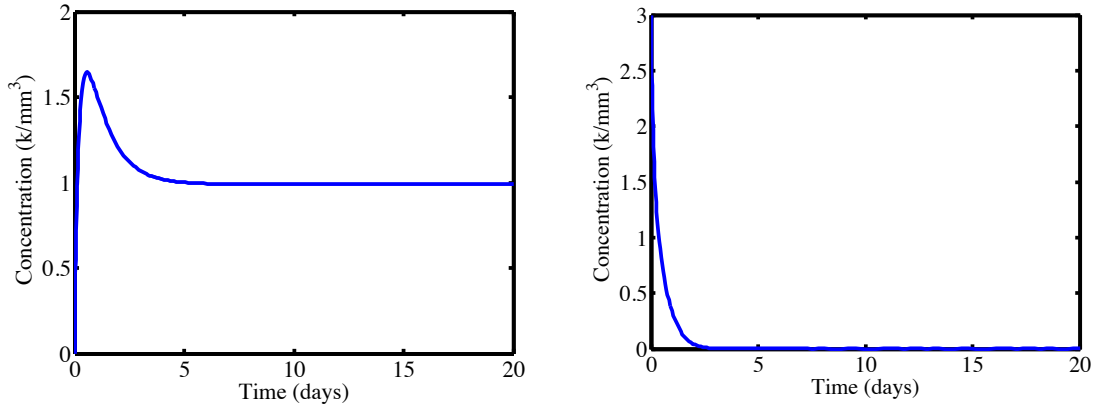
(a) Helper T cell deficient simulation: helper T cells. (b) Helper T cell deficient simulation: regulatory T cells.

Figure 2.9: Simulation of the initially helper T cell deficient system with initial conditions $H = 0$, $R = 3$.

2.5 Discussion

In this chapter, we developed a model of immune regulation and differentiation that is based on the biological study of [94]. The model considers helper T cells and regulatory T cells and highlights two recently accepted biological mechanisms: active suppression of helper T cells by regulatory T cells and the transition of regulatory T cells into helper T cells. Active suppression by regulatory T cells was shown to be a plausible mechanism of immune contraction as negative feedback provided by these cells was able to control immune expansion and return the system to homeostasis. Inclusion of the switching mechanism was shown to not disturb the expansion/contraction dynamics commonly displayed in immune models. This mechanism was shown to increase the robustness of the system, allowing for recovery from an imbalanced or even helper T cell deficient system.

We characterized the affects of Treg switching on the peak magnitude of the

immune response and identified the order of magnitude of the switching parameter, μ, that appears to be consistent with both the magnitude of the concentrations involved in an immune response and the ratio of Tregs to helper T cells.

The model can be extended in many directions. First, one can separate the dynamics between the lymph nodes and the site of infection. Under these conditions, one can investigate hypotheses such as those stating that only antigen induced Tregs in the periphery have the ability to become immuno stimulatory. Another extension will be to consider the case where only a certain percentage of Tregs may differentiate sideways. In Chapter 3, we use the knowledge gathered here to extend our study on the primary immune response by including both active T cell suppression and Treg switching in a more biologically detailed model of the regulation of the primary immune response.

Chapter 3

Modeling Adaptive Regulation with Regulatory T Cell Switching

3.1 Introduction

While the initial phases of T cell expansion are well understood (see [79]), the final contraction phase of the immune response is not. This contraction phase is crucial in bringing the immune system back to a stable state. Such a contraction must happen quickly to prevent damage to healthy cells and to prepare the system for future challenges. Hence, cell-mediated immune responses must be closely regulated following any antigenic stimulation.

Several key characteristics of the immune response should be considered when developing a model of these processes. Mercado *et al.* showed that T cell contraction and expansion were determined after 24 hours of exposure to a foreign antigen [75]. Kaech supported this by demonstrating that even with very short duration of exposure to antigen, cytotoxic T cells will divide $7 - 10$ times even after the antigen is removed [57]. Van Stipdonk observed that upon 20 hours of stimulation, naïve CD8+ T cells were able to carry out extensive proliferation and cytotoxic activity, characteristic of a fully developed immune response [108]. When combined together, experimental evidence suggests that the T cell response is mostly dictated in the first hours of antigen exposure and is therefore largely insensitive to the later characteristics of antigen exposure. A conclusion of these observations is that upon initial

37

activation by antigen exposure, T cells enter into an antigen-independent proliferation phase, known as a "T cell program". Mathematically, this has led to approaches rooted in a concept of T cell expansion wherein T cells enter a predetermined program where they divide for either a specified period of time or specific number of divisions [4, 58, 116]. The T cell response is also characterized in that it is robust to the precursor frequencies of antigen-specific naïve T cells. This is demonstrated by Badovinac *et al.* who showed that a 10,000-fold difference in antigen-specific T cell concentrations led to a mere 13-fold difference in peak of the CD8+ T cell response [7]. Mathematical models that address this data have been developed by Kim, Levy, and Lee [58, 59, 61] and will be discussed in further detail in Sections 3.1.1 and 3.2.

In this chapter, we construct mathematical models of the primary immune response taking into account the following biological observations:

- The T cell response is mostly determined in the first hours of antigen presentation [57, 75, 108].

- The T cell response is insensitive to precursor T cell frequencies [7].

- Regulatory T cells are the mechanism of contraction following pathogen clearance (see Section 2.2.1).

- Regulatory T cells have the ability to change their functionality and become immune promoting helper T cells [94].

In Section 3.1.1, we examine the characteristics of both division-based and time-based T cell programs and argue why neither hypotheses can account for the in-

herent robustness of the T cell response with respect to variations in the precursor frequency. In [58] and [59], Kim, Levy and Lee present a mathematical model of the immune response including adaptive regulatory T cells and show these cells they may play a crucial role in inducing a timely and robust contraction of the T cell response. In Section 3.2, we extend the models developed in [59] in light of the data presented in Chapter 2 to consider the affects of functional regulatory T cell switching. In 3.2.1, we define the related concept of immunodominance and discuss an extension of the immunodominance model of [59]. In Section 3.3, simulations of this model are shown and its robustness is demonstrated. Concluding remarks are given in Section 3.4.

3.1.1   T Cell Programs

Initial models of the dynamics of the immune response were based on predator-prey type dynamics wherein immune cells acted as predators and pathogens served the roll of the prey (see [2] for example). These models are able to generate some of the general features of the immune response such as expansion/contraction dynamics. However, they fail to exhibit some key experimentally-obtained features of the immune response. For example, these models do not show robustness to precursor frequencies or the ability to maintain an immune response after pathogen clearance.

The concept of a T cell program has been put forth to address the issue of antigen independence. In general, models developed under this paradigm describe the cell-mediated immune response as having a period of antigen-independent prolifera-

tion and a period of antigen-dependent proliferation that is followed by contraction that is determined by one of the theories mentioned in Section 2.2.1 (time-based, division-based, active suppression). These models are more consistent with experimental data concerning the antigen independent characteristics of the immune response shown in [57], [75] and [108].

In [4], Antia *et al.* develop models of the primary T cell response to acute infections. First, a model of antigen-independent T cell proliferation is considered. The T cell response is modeled as follows: upon initial antigen stimulation, CD8+ T cells progress through a *fixed* program of expansion, contraction and differentiation into memory cells. Further exposure to antigen does not alter the response. An alternative paradigm developed in this paper is one in which stimulated T cells undergo a short period of antigen-dependent expansion before entering an antigen-independent program. This model exhibits the expected basic expansion/contraction dynamics. This choice of technique for modeling antigen-independence has two noteworthy consequences. First, the model shows the ability to continue an immune response after removal of the antigen. This aligns with the experimental data of Kaech, Mercado and van Stipdonk [57, 75, 108]. However, as noted in [58], the antigen-dependent and antigen-independent parts of Antia's 2003 model occur in the opposite order of the more common notion that a developmental program precedes antigen-dependent proliferation as suggested in [57]. Furthermore, this arrangement of proliferation implies that the cell programming process takes approximately 2.5 days which contradicts van Stipdonk who proposes a 20 hour programming period [109, 108] and the 24 hour programming period proposed by Mercado [75]. Second, as observed

by Kim *et. al.*, a fixed program of expansion predicts that the magnitude of the response is directly proportional to the initial number of antigen-specific precursor T cells [58]. Hence, the Antia model contradicts the findings of Badovinac, which show that the magnitude of the immune response is largely insensitive to T cell precursor frequencies [7].

Wodarz and Thomsen developed a mathematical model in which antigen-independent cell divisions occur prior to antigen-dependent proliferation. In this model, activated T cells undergo a fixed number of divisions before differentiating into effectors and then into memory cells [116]. If infection persists, memory cells recycle back into the effector state and enter another round of divisions, repeating the program as many times as necessary. Consistent with experimental studies, the study of this model concluded that the optimal fixed division program entails 7 – 10 divisions. However, contrary to experimental studies, cells cannot return to the effector state without committing to the entirety of the T cell program. This could lead to a protracted response possibly leading to damage to healthy cells.

Models derived under either time or division-based proliferation programs typically generate robust responses to antigen availability but scale with respect to precursor frequencies. As an alternative to these approaches, Kim *et al.* develop a model under the hypothesis that the contraction of the immune response is governed by a preprogrammed initial activation phase that is augmented by adaptive regulatory mechanisms [58]. The authors present a model where T cell contraction is not uniquely determined by a predetermined program, but comes about as the result of negative feedback loops through interactions with regulatory T cells. In

this model, CTLs enter a "minimal development program" in which they commit to proliferation. This program initiates upon activation by antigen presenting cells and represents the antigen-independent portion of the immune response. After the minimal development program, if a cell receives further stimulation, it undergoes singular cell division, representing the antigen-dependent portion of the process.

When compared with both the cell-division and time-based predetermined T cell programs, the model of Kim *et. al.* displays a robustness to T cell precursor frequencies that is more consistent with the experimental studies of [7]. A 4 order of magnitude difference between naïve T cell frequencies reduces to a three order of magnitude difference in effector T cell peaks. The reduction in scaling is much closer to experiments than the direct scaling which is inherent to autonomous T cell programs. Hence, the model of Kim *et. al* demonstrated that such an approach produces a primary T cell response that is robust to both antigen stimulation and precursor frequencies.

In [58], the regulation of cytotoxic T cells was considered. The T cell population was not divided into helper T cells and CTLs. The model was extended in [59] and [61] to consider the regulation of helper and cytotoxic cells separately. This added measure of biological accuracy is consistent with our current theory of immune regulation and amenable to a consideration of regulatory T cell switching. Hence, our starting point is the model of [59] which we extend to incorporate our work on regulatory T cell stability developed in Chapter 2 into more comprehensive models of regulation.

3.2 A Mathematical Model of Adaptive Regulation with Treg Switching

The work presented here is based on the "Extended model of adaptive regulation: helper and killer T cells" presented in [59]. In this model, the immune reaction is modeled as a system of delay differential equations. The delay is derived from the notion that upon activation, a cell will spend a specified amount of time solely devoted to mitosis (cell division) before it can properly execute its functions. This model also considers the production and consumption of the pro-inflammatory cytokine IL-2. Consistent with current knowledge of T cell lineage, regulatory T cells differentiate from the helper T cell population and are able to suppress both helper and cytotoxic T cells [94]. The model is consistent with the theory of active suppression, displays many inherent immune characteristics (antigen and T cell precursor-independence), and thus provides an excellent framework within which to consider Treg switching. In our work, we use the work of [59] as the basic model to which we add terms to allow for regulatory T cell switching. Our model is described as follows (illustrated in Figure 3.1):

1. Upon encountering antigen, $a(t)$, immature APCs, $A_0(t)$, become mature APCs, $A_1(t)$, and migrate to the lymph node.

2. Naïve helper and cytotoxic T cells ($H^0(t)$ and $K^0(t)$, respectively) residing in the lymph nodes encounter mature APCs and enter a minimal developmental program in which they divide m_1 or m_2 times respectively.

3. Mature helper and cytotoxic T cells ($H(t)$ and $K(t)$, respectively) both secrete the positive growth signal IL-2, denoted $P(t)$.

4. Mature helper and cytotoxic T cells that have completed the minimal developmental program become effector cells that continue dividing upon further antigenic stimulation. This antigen dependent proliferation occurs in response to interactions with APCs for helper T cells and in response to IL-2 consumption for cytotoxic T cells.

5. In response to antigenic stimulation, some proportion of helper T cells further differentiate into Tregs, $R(t)$.

6. Regulatory T cells enact their feedback on the system by:

   - suppressing mature helper and cytotoxic T cells,

   - proliferating after consuming free positive growth signal,

   - transitioning back into the helper T cells at a rate that depends on the growth signals received from mature T cells.

1) Migration of APCs to lymph node

s_A A_0 $a(t)A_0$ A_1

2) Initial T cell activation

s_H H^0 A_1 $\dfrac{kA_1H^0}{delay = \sigma_1}$ $H \times 2^{m_1}$

s_K K^0 A_1 $\dfrac{kA_1K^0}{delay = \sigma_2}$ $K \times 2^{m_2}$

3) CD4+ and CD8+ T cells secrete positive growth signal (IL-2)

H r_1H P

K r_2K P

4) APC-driven proliferation of CD4+ cells. IL-2-driven proliferation of CD8+ cells & Tregs

H A_1 $\dfrac{kA_1H}{delay = \rho_1}$ $H \times 2$

P K $\dfrac{kPK}{delay = \rho_2}$ $K \times 2$

P R $\dfrac{kPR}{delay = \rho_1}$ $R \times 2$

5) CD4+ T cells differentiate into Tregs

H rH R

6) Tregs suppress effector T cells, and transition into helper T cells.

R H kRH ✗

K kRK ✗

R $\mu\dfrac{R}{1+dP}$ H

Figure 3.1: Diagram of the adaptive regulation with T cell switching model. The compartments are represented as follows: A_0: immature APCs, A_1: mature APCs, H^0: naïve helper T cells, H: mature helper T cells, K^0: naïve effector T cells, K: mature cytotoxic T cells, P: IL-2 cytokine, and R: regulatory T cells. Note that each compartment has an associated death rate, which is not represented in the diagram.

Our model of adaptive regulation with regulatory T cell switching is thus given by the following equations:

$$\dot{A}_0(t) = s_A - d_0 A_0 - a(t) A_0(t), \tag{3.1}$$

$$\dot{A}_1(t) = a(t) A_0(t) - d_1 A_1(t), \tag{3.2}$$

$$\dot{H}^0(t) = s_H - \delta_0 H^0(t) - k A_1(t) H^0(t), \tag{3.3}$$

$$\dot{H}(t) = 2^{m_1} k A_1(t - \sigma_1) H^0(t - \sigma_1) - k A_1(t) H(t) + 2k A_1(t - \rho_1) H(t - \rho_1)$$
$$+ \mu \frac{R(t)}{1 + dP(t)} - (\delta_H + r) H(t) - k R(t) H(t), \tag{3.4}$$

$$\dot{K}^0(t) = s_K - \delta_0 K^0(t) - k A_1(t) K^0(t), \tag{3.5}$$

$$\dot{K}(t) = 2^{m_2} k A_1(t - \sigma_2) K^0(t - \sigma_2) - k_E P(t) K(t) + 2k P(t - \rho_2) K(t - \rho_2)$$
$$- \delta_K K(t) - k R(t) K(t), \tag{3.6}$$

$$\dot{P}(t) = r_1 H(t) + r_2 K(t) - \delta_P P(t) - k P(t) K(t) - k P(t) R(t), \tag{3.7}$$

$$\dot{R}(t) = r H(t) + 2k P(t - \rho_1) R(t - \rho_1) - k P(t) R(t)$$
$$- \mu \frac{R(t)}{1 + dP(t)} - \delta_H R(t). \tag{3.8}$$

A_0 is the concentration of APCs at the site of infection and A_1 is the concentration of APCs that have matured and begun presenting antigen in the lymph node. The variable H_0 is the concentration of naïve helper T cells. H is the concentration of mature helper T cells. K_0 is the concentration of naïve cytotoxic T cells, K is the concentration of mature cytotoxic cells, and R is the concentration of Tregs. The growth signal, P, is the concentration of interleukin-2.

Equation (3.1) describes the immature APCs maintained throughout the body. There is a constant supply rate, s_A and proportional death rate, d_0. The invasion by an immunogen is represented by the rate, $a(t)$ defined by (2.3), with which the immunogen stimulates immature APCs to become mature APCs. The equation governing mature APCs in the lymph node is given by (3.2). The source of these cells is immature APCs that have been stimulated by antigen contact. These cells have a natural death rate of d_1.

Naïve T cell populations are described by Equations (3.3) and (3.5). Helper and cytotoxic T cells have a supply rate of s_H and s_K, respectively, and die at a proportional rate δ_0. Each of these populations mature at a rate proportional to their mass action interactions with mature APCs.

Equation (3.4) characterizes the mature helper T cell population. The first term gives the rate at which activated naïve helper T cells become mature upon completion of the minimal developmental program of m_1 cell divisions. The duration of this minimal developmental program is signified by the time delay σ_1. The second and third terms correspond to antigen dependent proliferation and represents the rate at which these cells are stimulated by mature APCs for further division. The time delay of ρ_1 is the duration of one CD4+ cell division. The fourth term describes the influx of helper T cells that have originated from regulatory T cells that have lost their suppressive capabilities. This term is one of the additions to the model of [59] due to the assumed Treg switching. Mature helper cells are removed from the system by three methods: natural death at rate δ_H, differentiation into Tregs at rate r, or by suppression due to interactions with Tregs.

47

Equation (3.6) governs mature CTLs. The first term of this equation gives the rate at which activated naïve CD8+ T cells enter the mature population after finishing the minimal developmental program of m_2 cell divisions. The duration of the minimal developmental program is given by the time delay σ_2. The second term is the rate at which these cells are stimulated by IL-2 for further division, and the third term is the rate at which cells reenter the mature CTL population after dividing once in the time period ρ_2. CTLs die naturally at a rate δ_K and are suppressed by Tregs.

The dynamics of IL-2 concentration are given by Equation (3.7). This cytokine is produced by mature helper and cytotoxic T cells at rates r_1 and r_2 respectively. The cytokine has a proportional decay rate, δ_P. The final terms of this equation describe the rates at which IL-2 is consumed by mature CTLs and Tregs.

The final equation, (3.8), describes the regulatory T cell compartment. The first term is the rate at which mature helper T cells differentiate into Tregs. The second and third terms describe the rate at which Tregs are stimulated by IL-2 for further division. Upon stimulation, Tregs are removed from the system at time, t, divide and return with a delay of ρ_1. The fourth term describes the rate of loss of regulatory function. As described in Section 2.3, this rate is dependent on the availability of IL-2. Lower values of $P(t)$ create higher rates of transition from regulatory to helper T cells while higher prevalence of $P(t)$ helps to sustain regulatory cells and decreases the rate of transition. Tregs also have a natural death rate δ_H.

3.2.1 A Model of Immunodominance with Treg Switching

In response to multiple epitopes (antigen molecules that the immune system recognizes), the immune response organizes into hierarchies in which the most dominant epitope elicits the most prominent T cell response. This phenomenon is known as *immunodominance*. If the most dominant epitope is removed, the second most dominant response may expand to compensate. Immunodominance hierarchies might change during subsequent presentations of the same antigen. The precise mechanisms of immunodominance are not well understood and there are two general schools of thought. Either T cells passively compete for resources (such as growth factors, access to APCs, etc.), or T cells actively suppress each other, leading to a structured response against the dominant epitopes [61].

There have been a number of mathematical models of immunodominance. For instance, the model developed in [81] shows that for an antigenically homogeneous virus population, there will be complete immunodominance, in which the immune system responds to only one epitope. This model also predicts that multiple immune responses against different epitopes can coexist. Kim *et al.* demonstrate how their model can be adapted to describe the phenomenon of immunodominance in [59]. A number of different scenarios are tested including, but not limited to, chronic antigen stimulation, knocking out dominant epitopes, and secondary immune responses. These simulations led to the conclusion that the determination of which epitope will result in the dominant T cell response depends on both precursor frequency and T cell reactivity to each epitope. Following [59], we extend our model (3.1) –

(3.8) to account for n distinct immune epitopes. This leads to the following model:

$$\dot{A}_0(t) = s_A - d_0 A_0 - a(t) A_0(t), \tag{3.9}$$

$$\dot{A}_1(t) = a(t) A_0(t) - d_1 A_1(t), \tag{3.10}$$

$$\dot{H}_i^0(t) = s_{H,i} - \delta_0 H_i^0(t) - k_i A_1(t) H_i^0(t), \tag{3.11}$$

$$\dot{H}_i(t) = 2^{m_1} k_i A_1(t - \sigma_1) H_i^0(t - \sigma_1) - k_i A_1(t) H_i(t) + 2 k_i A_1(t - \rho_1) H_i(t - \rho_1)$$
$$+ \mu \frac{R_i}{1 + dP} - (\delta_H + r) H_i(t) - k R_{total}(t) H_i(t), \tag{3.12}$$

$$\dot{K}_i^0(t) = s_{K,i} - \delta_0 K_i^0(t) - k_i A_1(t) K_i^0(t), \tag{3.13}$$

$$\dot{K}_i(t) = 2^{m_2} k_i A_1(t - \sigma_2) K_i^0(t - \sigma_2) - k_E P(t) K_i(t) + 2 k_i P(t - \rho_2) K_i(t - \rho_2)$$
$$- \delta_K K_i(t) - k R_{total}(t) K_i(t), \tag{3.14}$$

$$\dot{P}(t) = r_1 H_{total}(t) + r_2 K_{total}(t) - \delta_P P(t) - k P(t) K_{total}(t) - k P(t) R_{total}(t), \tag{3.15}$$

$$\dot{R}_i(t) = r H_i(t) + 2 k P(t - \rho_1) R_i(t - \rho_1) - k P(t) R_i(t)$$
$$- \mu \frac{R_i(t)}{1 + dP(t)} - \delta_H R_i(t). \tag{3.16}$$

Here, we consider T cell clones $i = 1...n$. For naïve T cells, mature T cells, and regulatory T cells, there is a separate equation for each epitope, denoted by the subscript i. Each clone has an individual kinetic rate, k_i. Although regulatory T cells are recruited with respect to a specific epitope, their suppressive activity is assumed not to be antigen specific. Thus, the suppressive terms are proportional to the mass action interactions with all regulatory cells, $R_{total} = \sum_{i=1}^{n} R_i$, regardless of the epitope of origin. Similarly, IL-2 is not epitope specific in its actions and the production of this cytokine is proportional to the total number of IL-2 producing

cells in the system and grows with respect to $H_{total} = \sum_{i=1}^{n} H_i$ and $K_{total} = \sum_{i=1}^{n} K_i$.

3.3   Results and Simulations

We solve equations $(3.1) - (3.8)$ numerically using Matlab's DDE solver, dde23. Parameter values for the model are given in Table 3.1. Most parameters were obtained from [59] to which we refer for full justification. The parameters for μ and d are approximated based on their contribution to the dynamics of the system. Figure 3.2 shows the evolution of the APC and CTL populations. Figure 3.2(a) demonstrates that immature APCs are able to mature within approximately 2.5 days of the initiation of the immune response. Consistent with the biological findings of [75] and [108], the entire naïve CTL population is recruited to participate in the immune response within 1 day of the start of simulation. Also, coinciding with experimental measurements showing that the T cell response peaks at 8 days after initiation [31], the simulation also demonstrates a peak CTL response at day 8.

We consider the consequences of positive and negative signals received by CTLs in Figure 3.3. Here we study how cytotoxic T cells behave relative to IL-2 and regulatory T cells. Initially, IL-2 levels rise due to the increase in the number of mature helper T cells (not shown). Further divisions past the minimal developmental program require the consumption of IL-2. Hence, as CTLs complete the minimal development program, they begin to consume IL-2, leading to a decrease in IL-2 concentration. Corresponding to the peak CTL response is the initiation of regulatory T cell proliferation. This rise in Tregs contributes to ending the CTL response in

	Description	Estimate
$A_0(0)$	Initial concentration of immature APCs	10
$H_0(0)$	Initial concentration of naïve CD4+ T cells	0.06
$K_0(0)$	Initial concentration of naïve CD8+ T cells	0.04
s_A	Supply rate of immature APCs	0.3
d_0	Death rate of immature APCs	0.03
b	Duration of antigen availability	10
c	Level of APC stimulation	2
d_1	Death rate of mature APCs	0.8
s_H	Supply rate of naïve CD4+ T cells	0.0018
s_E	Supply rate of naïve CD8+ T cells	0.0012
k	Kinetic coefficient	5
δ_0	Death rate of naïve T cells	0.03
δ_H	Death rate of mature helper T cells	0.23
δ_K	Death rate of mature cytotoxic T cells	0.4
m_1, m_2	Number of divisions in minimal development program for helper T cells and CTLs, respectively	$2, 7$
σ_H, σ_K	Duration of minimal developmental program for helper T cells and CTLs, respectively	$1.46, 4$
ρ_H, ρ_K	Duration of one T cell division for helper T cells and Tregs, respectively	$11/24, 1/3$
k_E	kinetic coefficient for CTL-Treg interactions	20
r_1	Rate of IL-2 secretion by mature helper T cells	10
r_2	Rate of IL-2 secretion by mature CTLs	1
δ_P	Decay rate of free IL-2	5.5
r	Rate of differentiation of helper T cells into regulatory T cells	0.02
d	magnitude of dependence of Treg switching on IL-2	10
μ	Rate of regulatory T cell switching	5

Table 3.1: Estimates of parameters for model (3.1) – (3.8). Concentrations are measured in k/mm^3. Time is measured in days. Initial conditions not explicitly given in the table are zero.

(a) Immature and mature APCs.

(b) Naïve and mature CTLs
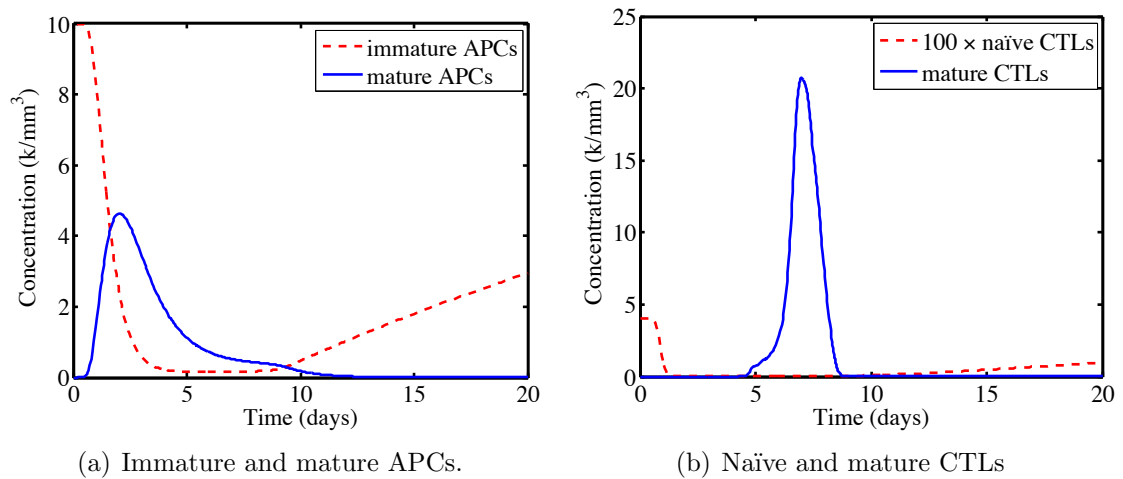
Figure 3.2: Simulation of (3.1) – (3.8) with parameters given in Table 3.1. The time evolution of antigen presenting cells and cytotoxic T cells are shown in Figures 3.2(a) and 3.2(b), respectively.
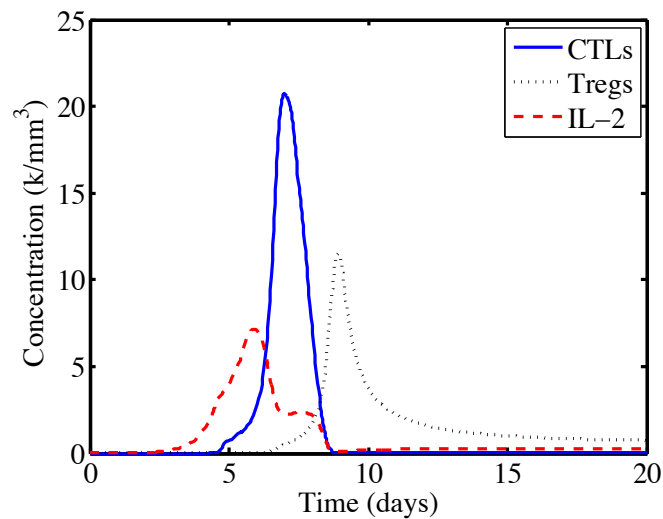
Figure 3.3: Time evolution of cytotoxic T cells, regulatory T cells and IL-2 in a simulation of (3.1) – (3.8) with parameters given in Table 3.1.

two ways. First, direct contact between Tregs and CTLs removes CTLs from the system. Second, because both Tregs and CTLs consume IL-2 as part of their division processes, competition for this cytokine reduces its availability, hindering the ability of CTLs to continue dividing.

We simulate the experiments of Badovinac in Figure 3.4. Here, we vary the
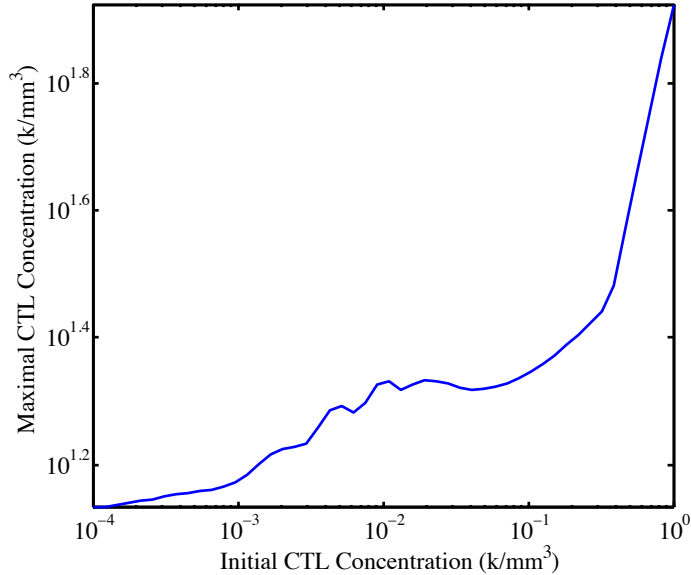
Figure 3.4: Numerical experiment reflecting the biological experiments performed by Badovinac in [7]. The maximal mature CTL concentration is considered as a function of the initial naïve CTL concentration.

concentration of initial naïve CTLs, $K^0(0)$, and note the maximum mature CTL concentration during the simulation. Similar to Badovinac, we perform this simulation over a group of initial concentrations ranging over 4 orders of magnitude. Our results show that over this range of initial concentrations, there is a change in peak response that varies by 1 order of magnitude. This is on par with the experimental results showing that a 10,000-fold change initial conditions led to a 13-fold change in peak response [7]. This is an improvement over the results of [59] in which a range

of 4 magnitudes in initial conditions led to a change of 3 orders of magnitude in peak response. We conclude that in comparison to the models presented in [59], the inclusion of Treg switching increases the system's robustness to initial conditions.

To study the impact of the regulatory T cell switching parameter, μ, on the dynamics of the system, we follow the techniques used to study equations (2.1) – (2.2) in Section 2.4. These results are shown in Figure 3.5. In Figure 3.5(a), we show the maximal number of CTLs as a function of μ. Unlike the results shown in Figure 2.8, this function of μ appears to be monotonic. However, it is clear that there is a more significant change in peak CTLs per change in μ for values of μ less than 5. We also consider the maximal ratio of Tregs to CTLs when choosing a value for μ. In Figure 3.5(b), we show the maximal Treg to CTL ratio as a function of μ. As discussed in Chapter 2, we expect this ratio to be in the range 0.1 – 1. We concentrate on ratios that lie in the center of this range and hence consider μ values between 4 and 10 (corresponding to ratios between .6 and .41).
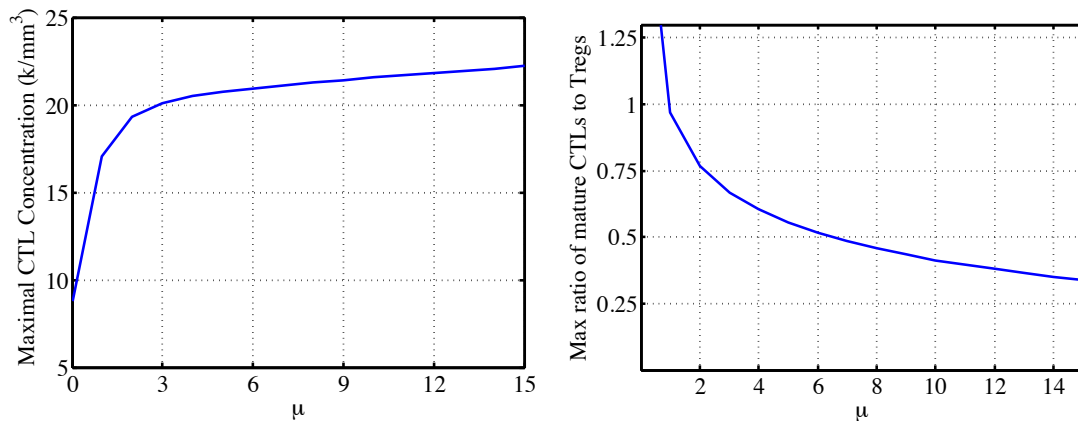
(a) Maximum cytotoxic T cell concentration as a function of μ.

(b) Maximum ratio of Treg to CTL concentration as a function of μ.

Figure 3.5: Graph depicting how the Treg switching rate, μ, affects the maximum CTL concentration (Figure 3.5(a)) and Maximum Treg to CTL ratio (Figure 3.5(b)).

3.3.1 Simulations of Immunodominace

We simulate equations (3.9) – (3.16) to consider multiple T cell clones (epitopes) responding to the same target at once. Each epitope is characterized by its reactivity to the target antigen, k_i, and its initial naïve CTL concentration, $K_i^0(0)$. The theory of immunodominance states that when faced with multiple epitopes, the immune system will primarily respond in accordance with a dominant epitope. If the most dominant epitope is removed (the so-called knock out experiment), then it is possible to have greater expansion of the less dominant epitopes to compensate for the missing epitope.

We simulate knock out experiments in Figures 3.6 and 3.7. The immune response to multiple clones is simulated by varying the initial CTL concentrations of the clones (Figure 3.6) or the reactivities (Figure 3.7). Epitopes are then "knocked out" one by one following the order of their dominance.

In Figure 3.6, we simulate four T cell clones, each with equal reactivities, $k_i = 20$ and initial concentrations: $K_1^0(0) = 0.04$, $K_2^0(0) = 0.01$, $K_3^0(0) = 2.5 \times 10^{-3}$, and $K_4^0(0) = 6.25 \times 10^{-4}$. Figure 3.6(a) shows a simulated immune response to all four clones. The response falls into a hierarchy based on the initial T cell concentration with Clone 1 remaining most dominant and Clone 4 remaining the least dominant. Figure 3.6(b) shows the result of a single knock out, in which Clone 1 is no longer a part of the simulation. Again, the immune response falls into a hierarchy dependent on initial concentration. Of interest is the fact that the response to Clone 2 almost quadruples when compared to the response elicited by Clone 2 in Figure 3.6(a).
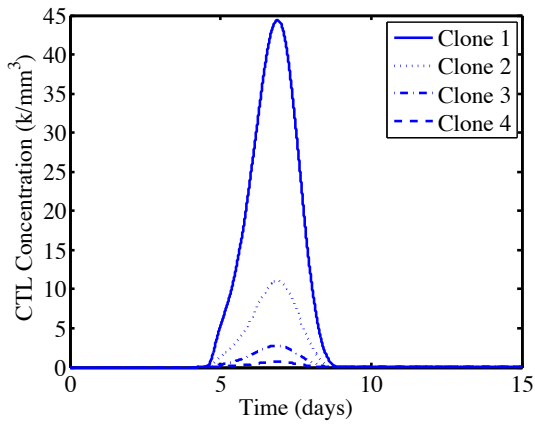
(a) All four clones: Clones 1,2,3 and 4.
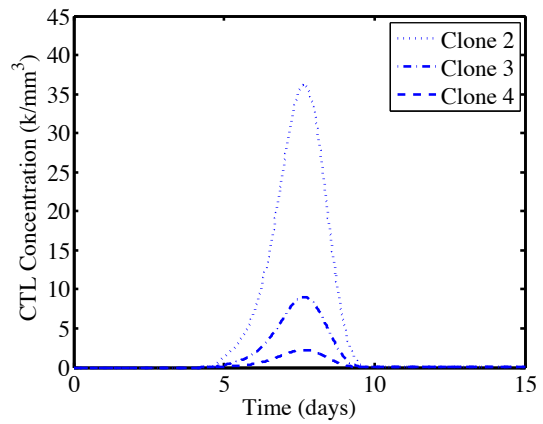
(b) Single knock out: Clones 2,3 and 4.
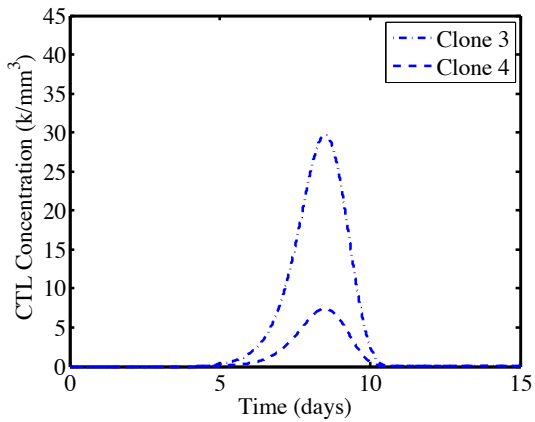
(c) Double knock out: Clones 3 and 4.
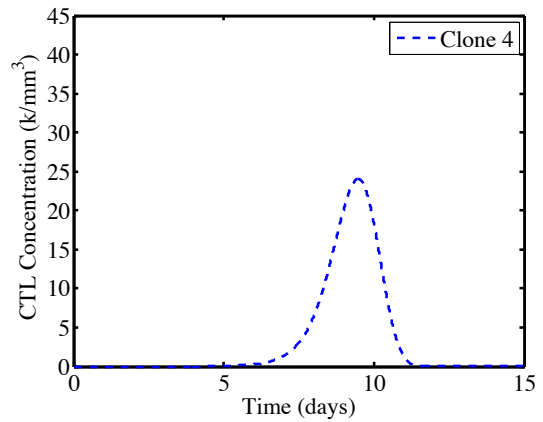
(d) Triple knock out: Clone 4, alone.

Figure 3.6: Simulated knockout experiment for four T cell clones. Each clone has equal reactivity, $k_i = 20$. Initial concentrations are: $K_1^0(0) = 0.04$, $K_2^0(0) = 0.01$, $K_3^0(0) = 2.5 \times 10^{-3}$, and $K_4^0(0) = 6.25 \times 10^{-4}$.

(a) All four clones: Clones 1,2,3 and 4.

(b) Single knock out: Clones 2,3 and 4.

(c) Double knock out: Clones 3 and 4.

(d) Triple knock out: Clone 4, alone.
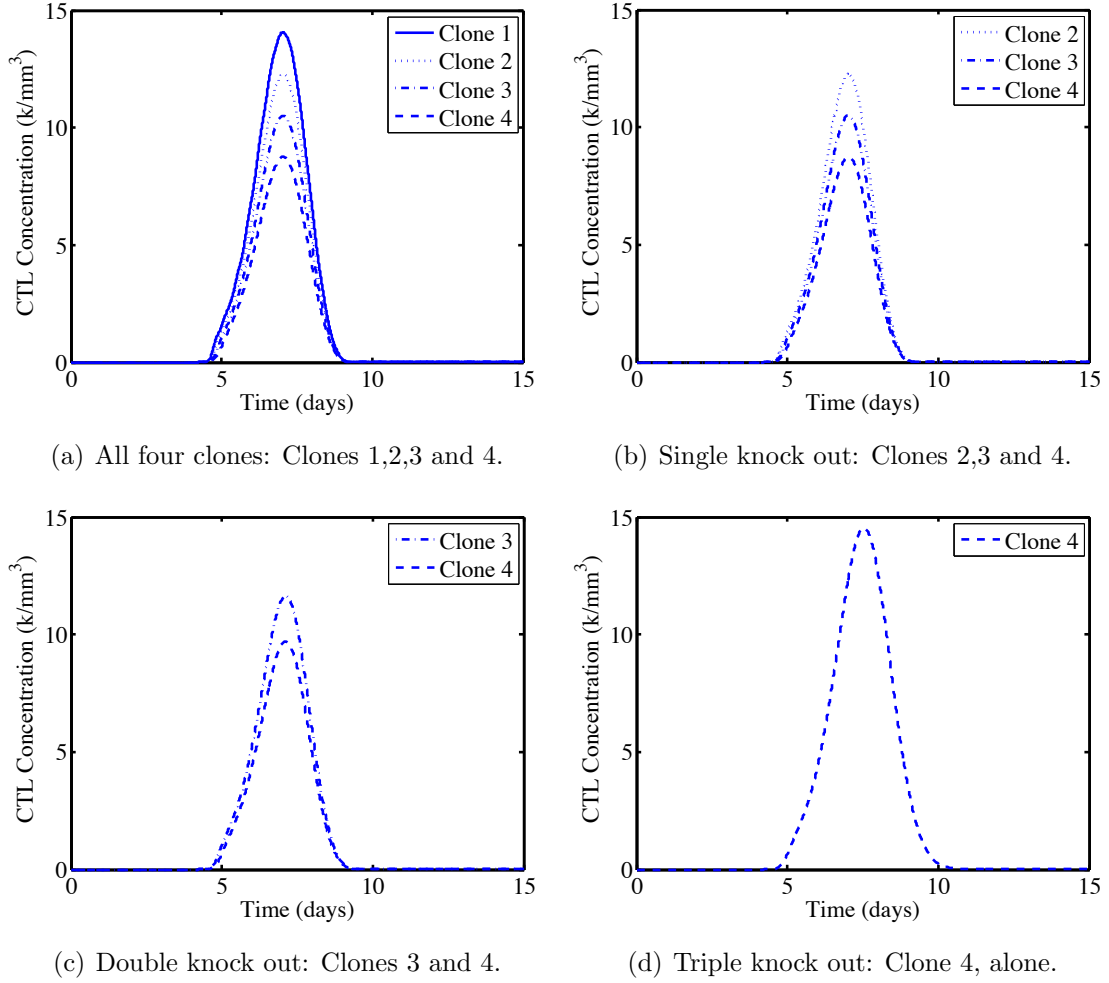
Figure 3.7: Simulated knockout experiment for four T cell clones. Each clone has equal initial concentration, $K_i^0(0) = 0.01$. Reactivities for clones are: $k_1 = 40$, $k_2 = 20$, $k_3 = 10$, $k_4 = 5$.

Despite the an initial concentration four times less that Clone 1, if Clone 1 is absent, the response to Clone 2 is able to compensate and produce a robust response similar in both timing and magnitude to the response garnered by Clone 1 in Figure 3.6(a). Similarly, if Clones 1 and 2 are removed, Clone 3 is able to compensate with a 10-fold increase in response in Figure 3.6(c) when compared to Figure 3.6(a). For Clone 4, when Clones 1,2 and 3 are removed, the response is approximately 25 times stronger in Figure 3.6(d) when compared to 3.6(a).

Figure 3.7 shows simulations for a knockout experiment in which each epitope

has the same initial concentration, $K_i^0(0) = 0.01$ and varying reactivities of $k_1 = 40$,

$k_2 = 20$, $k_3 = 10$, and $k_4 = 5$. We want to consider how this variation in reactivities

effects knock out experiments. Figure 3.7(a) shows a simulated immune response to

all four clones. As expected, the response falls into a hierarchy based on the initial

T cell concentration with Clone 1 being the most dominant and Clone 4 being the

least. A single knock out of Clone 1 is simulated in Figure 3.7(b). Different than

the knock out simulation in Figure 3.6(a), there is no clear compensation from any

of the remaining clones. Reactions to Clones 2, 3, and 4 are minimally increased

in Figure 3.7(b) than in Figure 3.7(a). Similar results are seen in Clones 3 and 4

when Clones 1 and 2 are removed (Figure 3.7(c)). Interestingly, the triple knock out

simulation does lead to Clone 4 expanding to compensate for the missing epitopes.

In fact, the response to Clone 4 alone (Figure 3.7(d)) is stronger than the response to

all four clones (Figure 3.7(a)). This suggests that, in the case of varying reactivities,

the relations that define immunodominant hierarchies may be more complex than

the linear scaling suggested in [59].

We continue our study of the effects of Treg switching on immunodominance

in Figure 3.8. As in Figure 3.6, we consider again the knock out experiment with

equal reactivities and varying initial T cell concentrations. To characterize the effects

of Treg switching, we consider the same knock out experiments for different Treg

switching magnitudes ($\mu = 2$, $\mu = 4$, and $\mu = 6$). As expected from our previous

study, increasing the value of μ increases the magnitude of the peak response of

CTLs. Also, for each value of μ considered, there is significant expansion of less
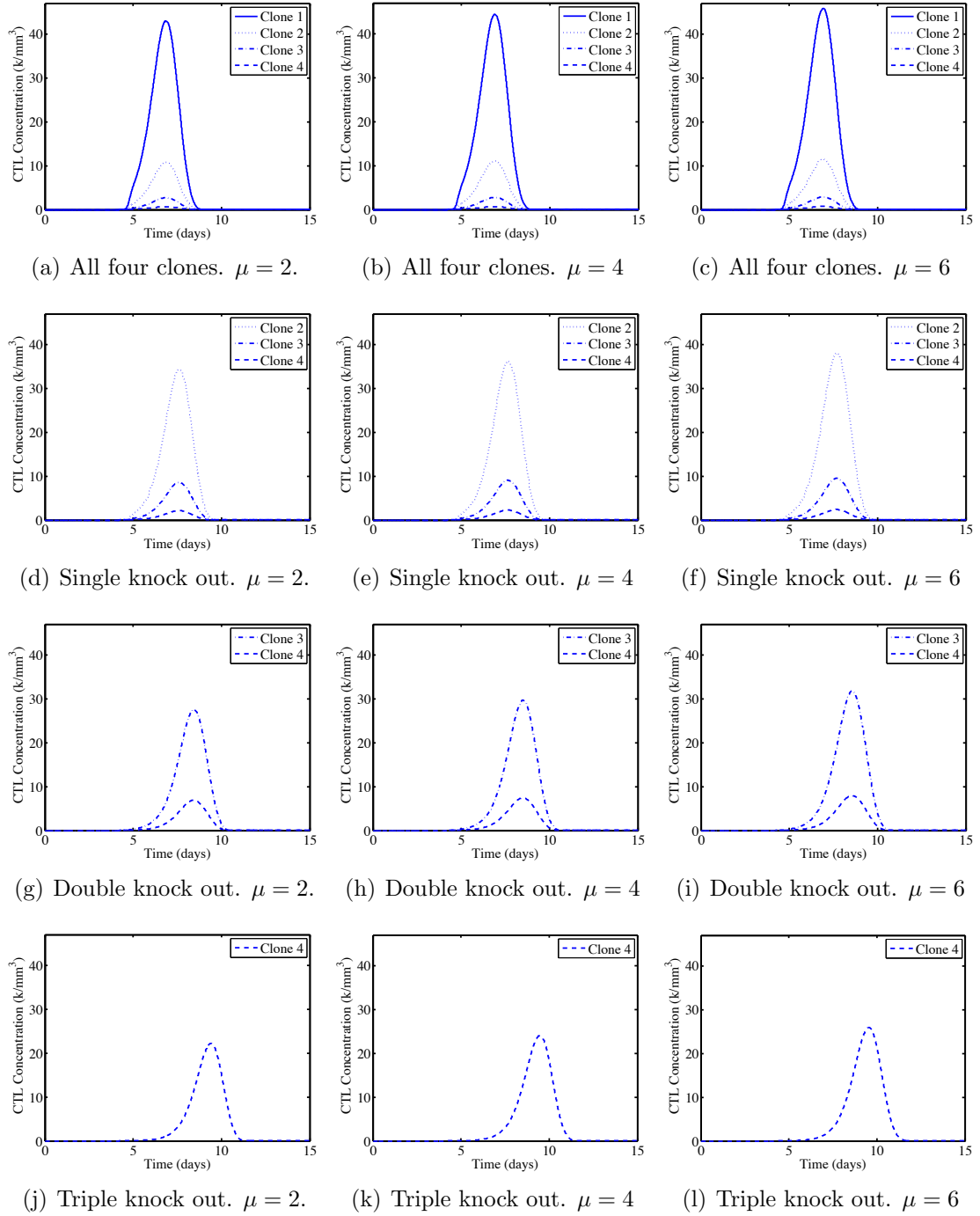
Figure 3.8: Simulated knockout experiment for four T cell clones. Each clone has equal reactivity, $k_i = 20$. Initial concentrations are: $K_1^0(0) = 0.04$, $K_2^0(0) = 0.01$, $K_3^0(0) = 2.5 \times 10^{-3}$, and $K_4^0(0) = 6.25 \times 10^{-4}$. Simulations are shown for $\mu = 2$ (left), $\mu = 4$ (center), and $\mu = 6$ (right).

dominant epitopes to compensate for the removal of more dominant epitopes. We take a closer look at the effects of μ on the ability of T cell clones to expand in such an experiment in Table 3.2. Here, for each clone and value of μ, we consider the peak CTL concentration when that clone is the most dominant epitope. We then divide by the peak response of the same clone when it is the least dominant epitope. We term this the "multiplicative expansion factor". This factor characterizes the ability of a clone to expand and compensate upon becoming the most dominant epitope. As expected, comparing values across the columns of Table 3.2 shows that less dominant epitopes have a greater capacity to compensate for knocked out epitopes. Comparing values down each column characterizes how μ affects the ability of a particular clone to expand. It is interesting to note that for the same clone, μ appear to increase the ability of the T cell clone to expand. For example, Clone 4 is capable of a larger expansion when $\mu = 6$ when compared to its expansion when $\mu = 2$.

	Multiplicative Expansion Factor		
μ	Clone 2	Clone 3	Clone 4
2	3.19	10.27	33.05
4	3.25	10.69	34.68
6	3.31	11.08	36.24

Table 3.2: Multiplicative expansion factors for the simulations shown in Figure 3.8.

We now study the effects of Treg switching in the case of varying cell reactivities. The results are shown in Figure 3.9. We consider knock out experiments for

different Treg switching magnitudes ($\mu = 2$, $\mu = 4$, and $\mu = 6$) and Clones $1 - 4$ with reactivities $k_1 = 40$, $k_2 = 20$, $k_3 = 10$, and $k_4 = 5$, respectively. As expected from our previous study, the effects of removing a clone are minimal for all but the triple knock out simulation. The multiplicative expansion factor for these simulations is given in Table 3.3. The multiplicative factors for Clones 2 and 3 indicate that little immune compensation takes place during these simulations. In particular, for $\mu = 2$ and $\mu = 4$, the expansion factor of less than 1 implies that the response to Clone 2 decreases in response to removing Clone 1. However, consistent with the results shown in Table 3.2, increasing μ also increases the expansion factor of a clone, although not as significantly as in the cases shown in Table 3.2.

|	Multiplicative Expansion Factor		
μ	Clone 2	Clone 3	Clone 4
2	0.98	1.07	1.53
4	0.99	1.10	1.65
6	1.00	1.14	1.80

Table 3.3: Multiplicative expansion factors for the simulations shown in Figure 3.9.
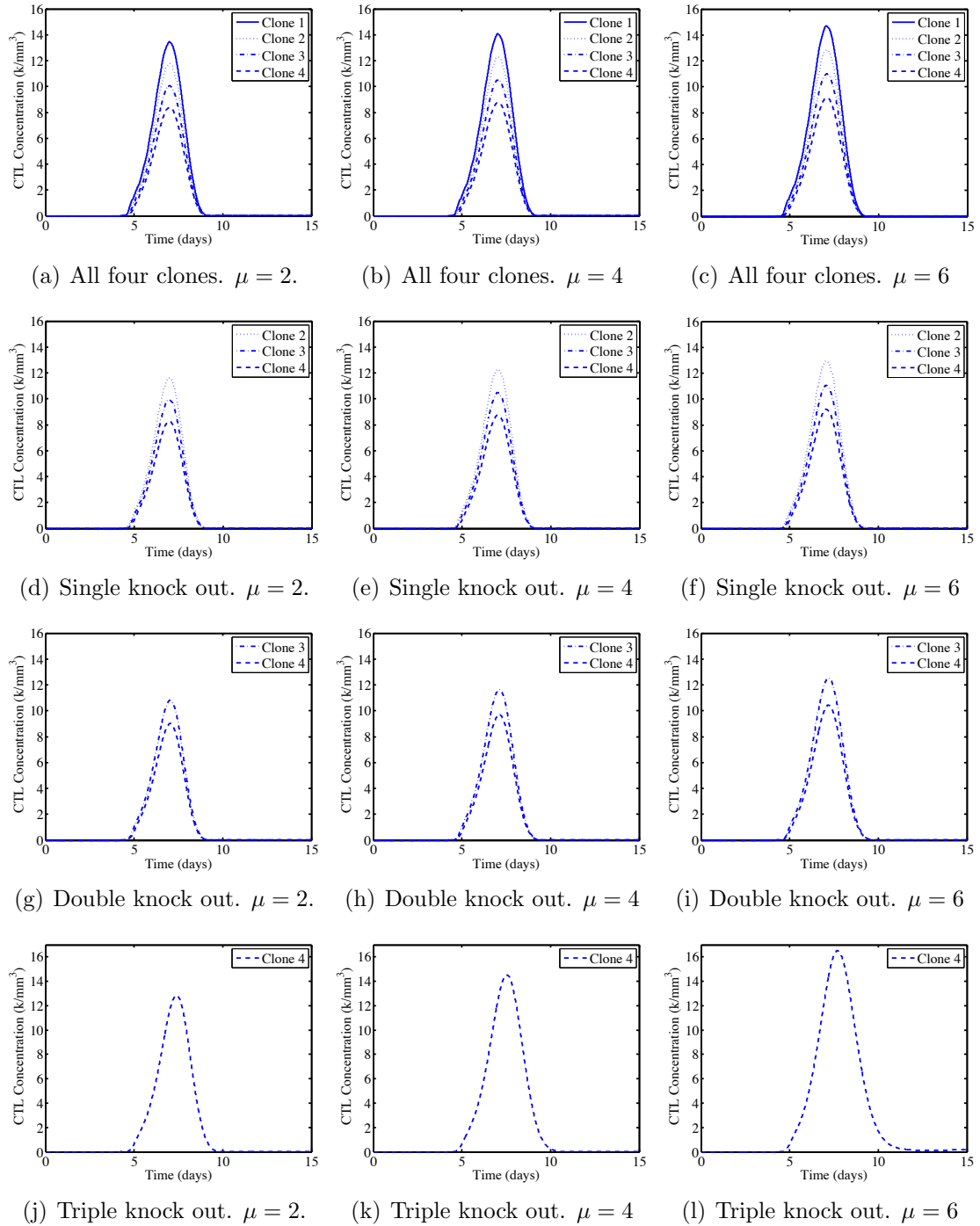
Figure 3.9: Simulated knockout experiment for four T cell clones. Each clone has equal initial concentration, $K_i^0(0) = 0.01$. Reactivities for clones are: $k_1 = 40$, $k_2 = 20$, $k_3 = 10$, $k_4 = 5$. Simulations are shown for $\mu = 2$ (left), $\mu = 4$ (center), and $\mu = 6$ (right).

3.4 Discussion

In this chapter, we extended the work presented in Chapter 2 concerning immune regulation and regulatory T cell switching. In this work, we added a mechanism of Treg switching to the DDE model of [59]. The basic principles of regulatory T cell switching described in Chapter 2 were shown to hold within the context of this more complex model and the addition of this mechanism was shown to improve certain aspects of the immune response studied in [59]. An improvement of this model over past models of the immune response was seen when considering how the immune response scales with respect to initial T cell concentrations. Consistent with biological experiments, varying initial T cell concentrations over 4 orders of magnitude led to a change in the peak immune response that varied by 1 order of magnitude. Also, consistent with results found in Chapter 2, we were also able to identify a plausible range for the rate of Treg switching, μ. Further experiments on the rates of Treg switching could contribute to obtaining a more accurate approximation of this value.

This model was also used to study the phenomena of immunodominance. Immune responses to multiple epitopes were shown to be able to coexist. Although the response to the most dominant epitope was shown to suppress the response to other epitopes, this model does not exhibit the winner-take-all dynamic that is seen in some mathematical models of immunodominance (see [81]). Knock out experiments were numerically simulated in two scenarios; one in which T cell clones vary in their initial concentrations and another in which they vary in cell reactivities. Immune

compensation of one epitope in response to the removal of a more dominant epitope was seen in the case of T cell clones with varied initial concentrations. In the case of varied cell reactivities, immune compensation was only seen in the triple knock out simulation. This suggests that further study is required in order to determine the relationship between cell reactivity and immunodominance hierarchies. An investigation of the effects of μ on immunodominance hierarchies showed that increasing μ not only increases the magnitude of immune response, it also increases the ability of T cell clones to expand within the immunodominance hierarchy.

Chapter 4

The Enhancement of Tumor Vaccine Efficacy by Immunotherapy

4.1 Introduction

Current cancer therapies predominantly focus on surgery, chemotherapy and radiotherapy; each of which carries major side-effects. The immune system is not always efficient in providing an adequate response to cancer, since cancer cells may not be easy to identify, and they use various immuno-suppression techniques to avoid the immune response (see Table 1.1). Recently, there has been an increased interest in improving the ability of the autologous immune response to target tumors, an approach that is generally being referred to as "immunotherapy."

Although animal models have demonstrated that humoral mechanisms may be relevant to immunotherapy, much of the promising work in tumor immunotherapy has been focused on T-cell-mediated, antigen-specific vaccines. Previous research has shown that through cellular immunotherapy, T cells can destroy large, established tumors [91]. Over the years, researchers have taken various approaches to tumor immunotherapy. Among these approaches are tumor cell-based vaccines, peptide-based vaccines, virus-based vaccines, DNA-based vaccines, and dendritic cells vaccines; each of which have met varying degrees of success at reducing or eliminating tumors (see the review papers [33, 91] and the references therein).

This work highlights how immunotherapy might be used to overcome the

effects of two regulatory agents exploited by cancer: regulatory T cells and the Transforming Growth Factor (TGF)-β protein. TGF-β is a protein that controls proliferation, cellular differentiation, and other functions in most cells. It acts as an anti-proliferation factor in normal epithelial cells [24]. Experimental evidence has shown that TGF-β can act as both a tumor suppressor and stimulator [86]. In early stages, it acts directly on cancer cells to suppress their growth. As the tumor progresses, TGF-β stimulates tumor progression by suppressing immune cells and promoting factors that contribute to tumor metastasis. High levels of TGF-β dampen the function and frequency of antigen presenting cells, cytotoxic T cells, and helper T cells. Also, TGF-β (in combination with IL-2) has been implicated in inducing an increased number of CD4+CD25+Fox3p+ regulatory T cells seen in tumors [44]. These regulatory T cells (Tregs) modulate the function of effector cells rendering them unable to continue their cytotoxic activity, leading to a weak or non-existent immune response to cancerous cells [14, 94].

The immunosuppressive effects of TGF-β on immune cells strongly support the development of TGF-β inhibitors to treat cancer. Several inhibitors of TGF-β are in various stages of development (see [44] and the references therein). Several clinical trials have evaluated TGF-β inhibition in cancer patients with some promising results. Unfortunately, while a few studies have shown the beneficial effects of anti-TGF-β in tumor treatment (see [9, 10]), Terabe *et al.* demonstrate that depletion of TGF-β is not always sufficient to elicit an effective immune response against cancerous cells [44, 106]. Using a mouse model, Terabe *et al.* showed that treatment with anti-TGF-β alone does not enhance the immune response. However, an

anti-TGF-β treatment did appear to facilitate an enhanced immune response when combined with an immune-boosting vaccine.

The goal of our present study is to understand part of the complex interplay between cancer, the immune system, and the immunoregulatory mechanisms that lead to ineffective immune responses. More specifically, we are interested in quantifying the effects that anti-TGF-β and vaccine treatments might have on the stability of the tumor-immune dynamic and how the combined treatment might contribute to tumor clearance as opposed to tumor escape. In order to understand how the suppression of regulatory mechanisms might affect a cancer vaccine, we develop a mathematical model to analyze the effects of anti-TGF-β treatment when used in conjunction with a vaccine as treatments for tumor growth. This is viewed as a step in developing a framework within which experimentalists may test treatment protocols prior to conducting their experiments. Our work is based on the experiments of [106].

A number of mathematical models have been developed to describe tumor-immune dynamics. A review of non-spatial tumor-immune models can be found in [38]. ODE models provide a framework within which one can explore the interactions among tumor cells and the alternate agents (such as immune cells, healthy tissue cells, cytokines, etc.). A general, non-spatial tumor-immune model considers an effector cell population (CTLs, NK Cells, etc.) interacting with tumor cells. In the earliest models, these interactions are described by two equations, where the immune cells play the role of the predator, while the tumor cells are the prey [69]. A framework for all such models is developed and analyzed in [36]. Many models

incorporate different immuno-therapeutic strategies such as injection of cytokines [22, 63], transfer of effector cells [63], or immunization with dendritic cells [23].

There are several mathematical models that specifically incorporate the effects of TGF-β on tumor development [20, 26, 67, 76, 89, 112]. One such model that considers the effects of TGF-β on tumor growth while also including a treatment that consists of constant infusion of exogenous CTLs is developed in [66]. The model developed in [62] specifically considers disrupting TGF-β production as a method of tumor treatment. Their mathematical model describes tumor growth, immune escape, and anti-TGF-β treatment. In contrast, this work mathematically studies a combined therapy through TGF-β inhibition and CTL vaccine.

The structure of this chapter is as follows: In Section 4.2.1, we describe the experimental background that was used as a basis for this work. In Section 4.2.2, we present an ODE model of tumor growth that is then used to investigate the effects of vaccinations and TGF-β inhibition. Model simulations and a stability analysis are included in Section 4.3. The main results for the four treatment regimes are shown in Figure 4.2. Closing remarks and directions for future work are given in Section 4.4. The results of this chapter were accepted for publication in the Bulletin of Mathematical Biology.

4.2 A Model of Tumor Vaccine Enhancement by TGF-β Inhibition

4.2.1 Biological Background

Our mathematical model is based on the experimental data presented in [106]. In this study, Terabe *et al.* examined whether TGF-β neutralization can potentiate immune responses caused by a CTL-inducing vaccine. Their goal was to determine the conditions under which this enhanced immune response inhibits and/or eliminates tumor growth in a TC1 mouse tumor model. This particular tumor line expresses the human papilloma virus (HPV) E6 and E7 genes (i.e. the tumor is slightly immunogenic) and manifests in lung epithelial cells. Twenty thousand cancer cells were injected into the right flank of the mouse and four days after tumor challenge, mice were immunized with HPV peptide. The TGF-β inhibitor used for experiments was 1D11; a murine anti-TGF-β monoclonal antibody that neutralizes all three isoforms of TGF-β. This antibody was shown to have minimal side effects in normal, tumor-free animals. The main results of [106] can be summarized as follows:

1. Blocking TGF-β enhances the effects of an anti-tumor peptide vaccine. In the case where both treatments were given, the tumor burden was significantly lower than any other treatment option tested; and 40% of mice remained tumor free for at least 55 days after tumor challenge.

2. Anti-TGF-β enhances the quantity and the quality of the vaccine-induced CD8+ CTL responses.

3. The enhancement of the immune response was shown to *not* be due to:

- suppression of CD4+CD25+ Tregs.

- suppression of IL-17 producing T cells.

- Natural Killer T cell-induced TGF-β production by Myeloid-derived Suppressor Cells.

The conclusion of the experimental study in [106] was that monotherapy with anti-TGF-β did not have a significant impact on tumor growth. The anti-TGF-β did, however, significantly enhance the efficacy of the peptide vaccine by inducing an increased number of tumor antigen-specific CTLs, which is critical for the effective elimination of tumors.

4.2.2 Mathematical Model

In order to quantitatively study the experimental setup of [106], we developed a mathematical model. In this model, we follow the dynamics of the tumor size, denoted $T(t)$; TGF-β concentration, denoted $B(t)$; activated cytotoxic effector cells, denoted $E(t)$; regulatory T cells, denoted $R(t)$; and vaccine-induced cytotoxic effector cells, denoted $V(t)$. A diagram of the different interactions between these elements is shown in Figure 4.1.
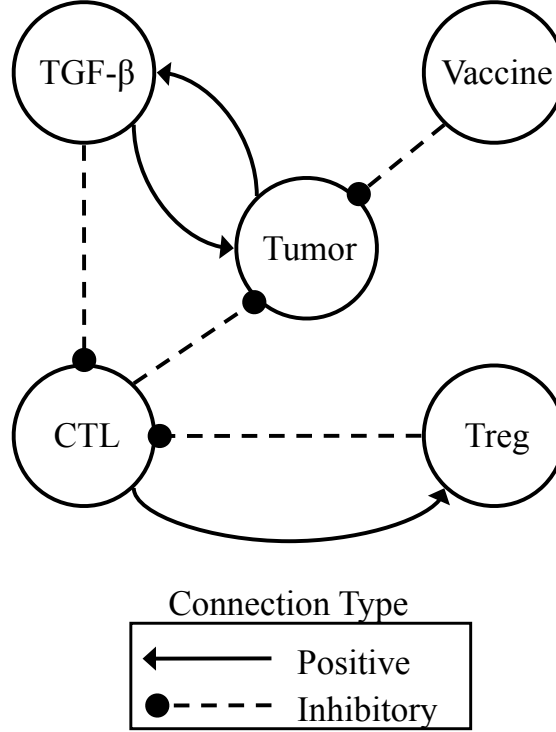
Figure 4.1: A diagram of the interactions between the different populations in the mathematical model of tumor vaccine and TGF-β inhibition.

Our mathematical model is written as the following system of ODEs:

$$\frac{dT}{dt} = a_0 T(1 - c_0 T) - \delta_0 \frac{ET}{1 + c_1 B} - \delta_0 TV, \tag{4.1}$$

$$\frac{dB}{dt} = a_1 \frac{T^2}{c_2 + T^2} - dB, \tag{4.2}$$

$$\frac{dE}{dt} = \frac{fET}{1 + c_3 TB} - rE - \delta_0 RE - \delta_1 E, \tag{4.3}$$

$$\frac{dR}{dt} = rE - \delta_1 R, \tag{4.4}$$

$$\frac{dV}{dt} = g(t) - \delta_1 V. \tag{4.5}$$

Equation (4.1) describes the tumor size measured in mm^2. The tumor follows logistic growth dynamics with growth rate, a_0, and carrying capacity, $1/c_0$. The

second term on the RHS of (4.1) describes the ability of immune cells to induce apoptosis of tumor cells. This clearance rate is inversely related to the amount of TGF-β present in the system (i.e. TGF-β diminishes CTL ability to induce apoptosis in tumor cells). The last term defines the action of vaccine cells on tumor cells. Since vaccine cells are considered to be fully differentiated, they are assumed to be unaffected by the inhibitory effects of TGF-β. Vaccine cells induce the death of tumor cells at a rate δ_0.

The dynamics of the concentration of TGF-β cytokine, measured in ng/ml, are described in equation (4.2). Experimental evidence has shown that TGF-β production by tumor cells is low for small tumors but "switches" on as the tumor grows; promoting immune evasion [83]. The use of equation (4.2) as a model for TGF-β production is described in [62]. As in [62], the maximum rate of TGF-β production is represented by the parameter a_1; c_2 is the critical tumor size at which the switch occurs; and the decay rate of the protein is d.

Equation (4.3) describes the dynamics of the number of effector T cells in the system. The first term represents immune recruitment. Effector cells are activated proportionally to the number of interactions with tumor cells. This term is multiplied by $(1 + c_3 T B)^{-1}$ to account for the combined negative effect of tumor growth and TGF-β production on immune recruitment and proliferation. The parameter c_3 represents the magnitude of the inhibition associated with tumor growth and TGF-β. A proportion, r, of effector cells differentiate into regulatory T cells (a process that is further discussed in the next paragraph). The final term of this equation models the removal of effector T cells from the system. These cells have both a

natural death rate; assumed to be the natural death rate for all effector cells, δ_1; and a death/removal rate that is proportional to the mass action interaction with regulatory T cells, δ_0. These magnitudes are assumed to be the same.

Equation (4.4) describes the number of Tregs in the regulatory T cell compartment. Though regulatory T cells originate from both CD4+ and CD8+ T cells [96], this model follows the principles of minimal design by considering only CD8+ effector T cells as precursors to Tregs. The feedback mechanism in this model applies as long as CTLs induce the production and/or recruitment of Tregs. A similar approach to simplifying the modeling adaptive regulation was taken in [58, 114].

In the model, Tregs differentiate from (or are recruited by) effector T cells at a rate r. The second term is the rate at which Tregs die. These cells provide negative feedback to the effector T cell population. Regulatory T cells should be considered as removing effector T cells from the system rather than killing them. While it is possible that effector T cells die upon interaction with regulatory T cells, that is not necessarily the only explanation. As suggested in [60], it is also possible that some effector cells might turn into memory cells, some might lose their effector function, and others might migrate away from the lymph node and carry out effector functions in the periphery. For the purposes of the model, suppressed cells, cells that have migrated, and dead cells are irrelevant to the dynamics, so we consider them all to be removed from the system.

Equation (4.5) describes the vaccine. The vaccine is modeled as an influx of activated tumor-specific cytotoxic T cells. These cells are impulsively introduced into the system at day 3 and are considered to be fully differentiated (i.e. no longer

dividing). If the vaccine is given,

$$g(t) = g_0 \delta(t - 3),$$

where $g_0 = 5,000$ and $\delta(t)$ is the Dirac delta function. If the vaccine is withheld,

$$g(t) \equiv 0.$$

Vaccine cells have a natural death rate of δ_1. This aspect of the model deviates from the experimental setup. In the experiment, a peptide vaccine is given to induce the production and proliferation of CTLs, while here, we model the vaccine as a direct injection of CTLs. The model vaccine is more in line with vaccination through adoptive T cell transfer, and therefore, might make the model more adaptable to experiments involving less antigenic tumors. Some of the consequences of this design decision will be discussed in the Sections 4.3 and 4.4.

4.3   Results

In our simulations we consider the following four scenarios:

a. no treatment

b. vaccine treatment

c. anti-TGF-β treatment

d. combined anti-TGF-β and vaccine treatment.

Parameter	Units	Description	Estimate	Source
a_0	day^{-1}	tumor growth rate	0.1946	fit to data [106]
$1/c_0$	mm^2	tumor carrying capacity	368.872042	fit to data [106]
δ_0	#$^{-1}$ day^{-1}	effector T-cell induced tumor death rate/ removal rate of CTLs by Tregs	1×10^{-5}	estimated
c_1	ml/ng	TGF-β inhibitory parameter for CTL induction of tumor death	100	estimated
a_1	days^{-1}ng/ml	maximal production rate of TGF-β	0.3	[62]
c_2	(mm^2)^2	steepness coefficient of TGF-β production	300	[62] or estimated
d	day^{-1}	degradation rate of TGF-β	7×10^{-4}	[62]
f	#$^{-1}$ day^{-1}	tumor antigenicity	0.62	estimated
c_3	ml / (ng mm^2)	combined tumor growth and TGF-β inhibitory parameter for activation of CTLs	300	estimated
r	#$^{-1}$	rate of effector T cells that become regulatory T cells	0.01	[58]
δ_1	day^{-1}	natural death of CTLs, Vaccine cells, and Tregs	1×10^{-5}	estimated

Table 4.1: Baseline control parameter values used in simulations of (4.1)–(4.4).

The list of the parameters used in our simulations is given in Table 4.1. The parameters a_0 and c_0 were approximated using a nonlinear least squares fit to the control data presented in [106]. Baseline values for a_1, c_2 and d were obtained from [62]. The value for the immuno-suppressive effects of TGF-β, c_1, was estimated based on data presented in [106]. The rate of effector cells that differentiate into regulatory cells, r, was given in [58] and falls in accordance with the range presented in [96]. A parameter sensitivity analysis was performed on the model parameters. The results of this analysis are presented later.

4.3.1 Simulations

Numerical solutions of (4.1)–(4.5) were obtained using Matlab's ODE23 solver. Starting with the initial measurements presented in [106], we begin our simulations at Day 3 after tumor presentation and conclude all simulations on day 30. At the initial time point, we assume that tumor antigenicity has led approximately 100 activated effector T cells to be present at the site of the tumor. This is consistent with the number of mouse precursor CTLs presented in [16] in which they estimated the number of D^b GP33-specific CD8 T cells to be 2×10^2.

Figure 4.2 shows results of our simulations in the four treatment regimes along with the corresponding experimental data. The simulation and the control data to which it was fit are shown in Figure 4.2(a). As previously mentioned, the control data set was used to approximate some of the model parameters. We calibrated the no-treatment model to follow the growth trend of the experimental data. While the

(a) No Treatment

(b) Vaccine Treatment

(c) TGF-β Inhibitor Treatment
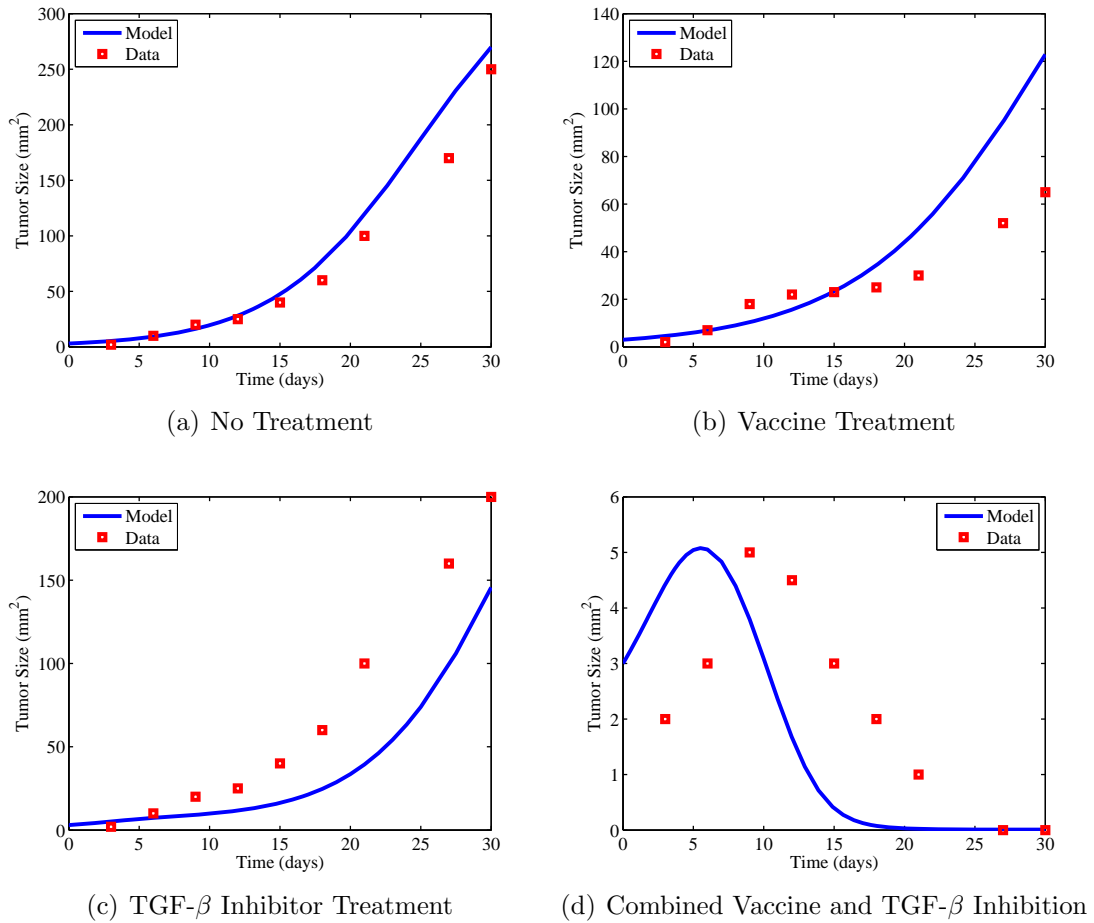
(d) Combined Vaccine and TGF-β Inhibition

Figure 4.2: The dynamics of the tumor size in four treatment regimes. Shown are the results of the numerical simulations along with the experimental data from [106]

precise timing of the observed phenomena is not captured by the present model, it is the qualitative aspects of the increase and decrease in the tumor size that we are seeking. The goal of this model is to capture the phenomena of tumor escape with monotherapy, and the peak tumor size and tumor eradication in the case of a combined therapy. These biological aspects are clearly captured by the current model.

In Figure 4.2(b), the vaccine treatment is modeled as an addition of $5,000$ effector T cells to the vaccine equation at day 3 of simulation. These cells are assumed to be resistant to TGF-β. In this case, there is a steady growth of the tumor throughout the simulation. The vaccine facilitates conditions that lead to a smaller tumor at the final time step. These cells do not multiply once added to the system, and hence the benefit of the vaccine slowly diminishes at the natural death rate for vaccine cells. This means that if the initial size of the vaccine is not large enough to overpower the tumor growth, then the tumor will always escape immunosurveillance.

We model TGF-β inhibition as an increase of c_2 from 300 to $7,000$. This effectively delays the "switch" of TGF-β production by approximately 8 days. The results of this simulation are shown in Figure 4.2(c). In this case, we see that the tumor remains small for the duration of TGF-β inhibition. However, soon after the TGF-β levels begin to recover, tumor growth quickly becomes uncontrolled. Similar results were seen for other values of c_2. In simulation, we see that singular TGF-β inhibition leads to a reduction in final tumor load at 30 days of simulation. This initial delay of tumor growth differs from the original data in [106], however the

final result of uncontrolled tumor growth remains similar.

The final case, Figure 4.2(d), shows the predictions of the model when both TGF-β and vaccine treatments are administered. Similar to the experimental results in [106], we see that a combined treatment is sufficient to induce tumor eradication. Model simulations lead to agreement with experiments concerning the peak tumor size. The timing of this maximum tumor size will be the addressed in the discussion. Simulations show an initial phase of tumor growth, but at approximately day 21, the immune system is able to clear the tumor. This suggests that such an outcome is the result of long-term presence of CTLs provided by the vaccine, in combination with the TGF-β inhibitor that provides an initial boost to the host's native immune system.

Figure 4.3 compares the tumor growth in all four treatment regimes. It is clear that while monotherapy results in a slowing down of the tumor growth, the tumor is still able to escape immunosurveillance and grow uncontrolled. Only in the case of dual therapy is the immune system able to eradicate the tumor.

We show the dynamics of the individual populations in the control case and the combined treatment case in Figure 4.4 and Figure 4.5. Figures 4.4(a) and 4.5(a) show how the tumor population changes over time. Figures 4.4(b) and 4.5(b) demonstrate the dynamics of the TGF-β concentration. In the no-treatment scenario 4.4(b), we see that the TGF-β levels are increasing with the tumor size. These high levels of TGF-β, particularly at later time points, contributes to the suppression of the effector T cell concentration as seen in Figure 4.4(c). In the combined treatment scenario, TGF-β levels are kept very low (see Figure 4.5(b)). This contributes to a
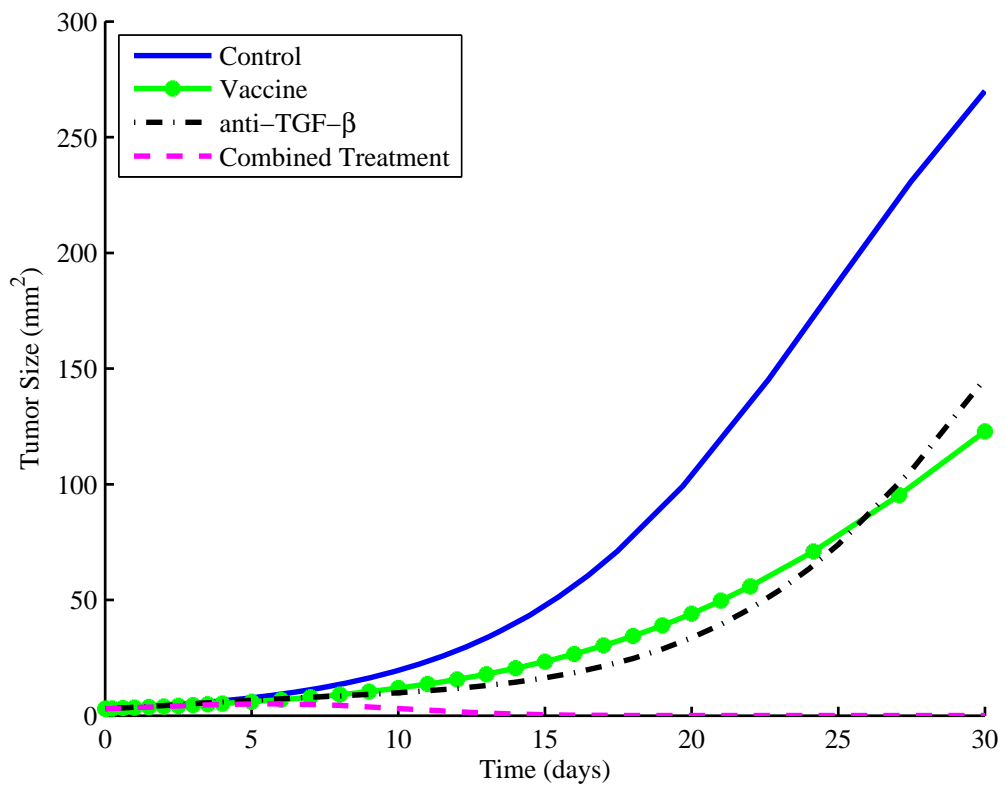
Figure 4.3: A comparison of the dynamics of the tumor size for all treatment regimes.
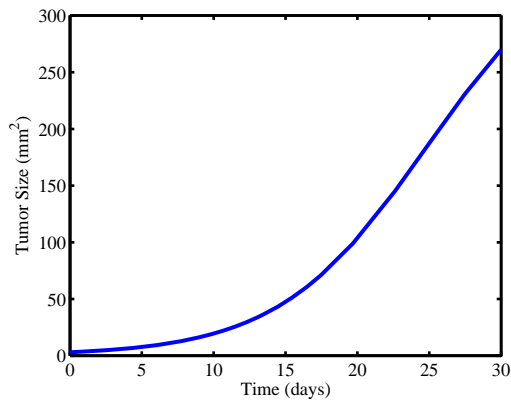
(a) No Treatment: Tumor Size
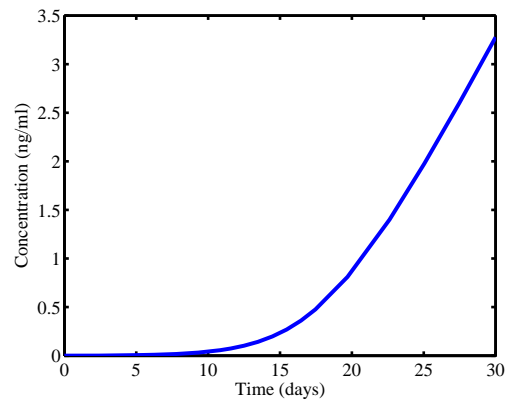
(b) No Treatment: TGF-β Concentration
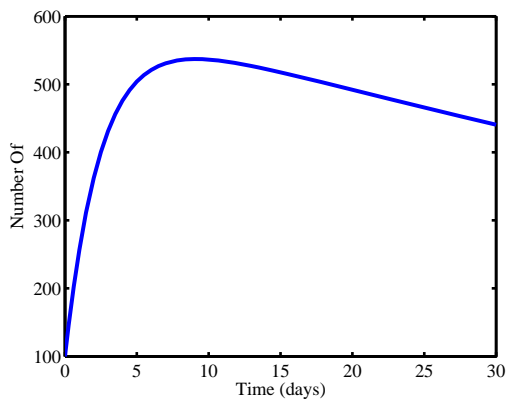
(c) No Treatment: CTL Population
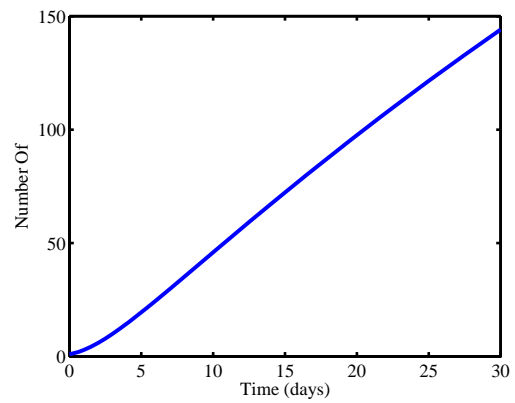
(d) No Treatment: Treg Population

Figure 4.4: Simulated population dynamics of the individual populations in the control case: (a) Tumor size (mm^2), (b) TGF-β concentration (ng/ml), (c) CTL population (number of), (d) Treg population (number of).
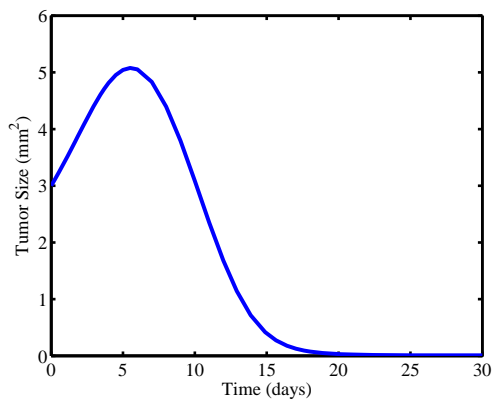
(a) Combined Treatment: Tumor Size
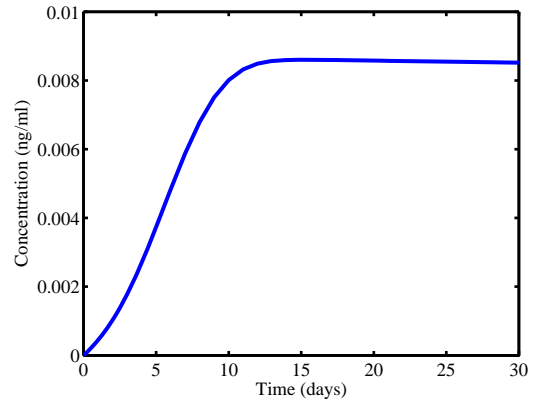
(b) Combined Treatment: TGF-β Concentration
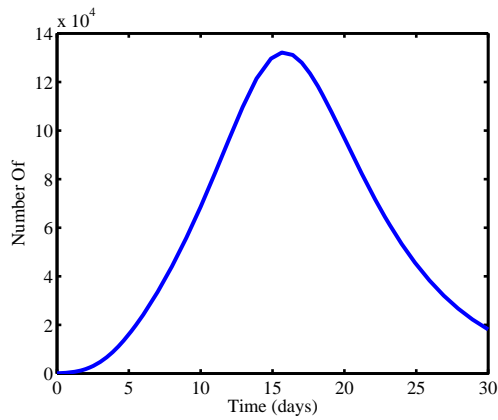
(c) Combined Treatment: CTL Population
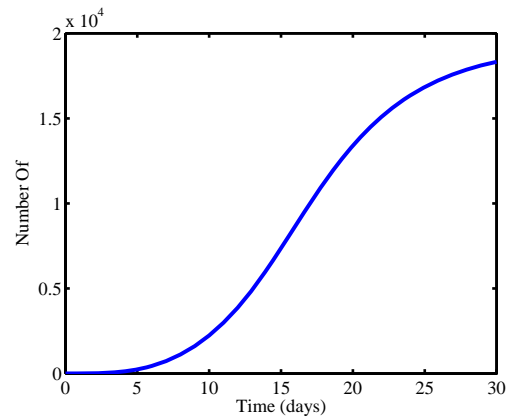
(d) Combined Treatment: Treg Population

Figure 4.5: Simulated population dynamics of the individual populations with combined treatment: (a) Tumor size (mm^2), (b) TGF-β concentration (ng/ml), (c) CTL population (number of), (d) Treg population (number of).

robust immune response peaking on Day 16 with just under $140,000$ CTLs present in the system (Figure 4.5(c)). The regulatory T cell populations are shown in Figures 4.4(d) and 4.5(d). Though these regulatory cells are effective at ending the immune response in both cases, the maximum ratio of regulatory cells to T cells is 0.075 in the no-treatment case and 0.062 in the case of a combined treatment. This aligns with the results of [106] which indicated that TGF-β inhibition does not suppress Treg production, but it does increase the ratio of effectors to Tregs in each of the treatment scenarios.

4.3.2   Equilibrium Analysis

We solve for the steady states of the control system by the usual manner of setting the left hand sides of (4.1) – (4.4) equal to 0 and solving for T, B, R, and E. The calculation for this is shown below.

We begin with the following system:

$$0 = a_0 T(1 - c_0 T) - \delta_0 \frac{ET}{1 + c_1 B}, \tag{4.6}$$

$$0 = a_1 \frac{T^2}{c_2 + T^2} - dB, \tag{4.7}$$

$$0 = \frac{fET}{1 + c_3 TB} - rE - \delta_0 RE - \delta_1 E, \tag{4.8}$$

$$0 = rE - \delta_1 R. \tag{4.9}$$

Case 1 $T = 0$ *or* $B = 0$:

A simple consideration of (4.7) shows $T = 0 \Leftrightarrow B = 0$.

From (4.9), we get

$$0 = rE - \delta_1 R,$$

$$i.e., \ E = \frac{\delta_1}{r} R. \tag{4.10}$$

Combining $T = B = 0$ with equations (4.8) and (4.10), we obtain

$$0 = \frac{-\delta_1}{r} R(r + \delta_0 R + \delta_1).$$

Hence, in Case 1, steady states will arise from two possible sub-cases: $R = 0$ or $r + \delta_0 R + \delta_1 = 0$.

Case 1.1 $R = 0$.

From (4.10) it follows that $R = 0 \Leftrightarrow E = 0$. Hence, we have the all zero solution of $T = B = E = R = 0$.

Case 1.2 $r + \delta_0 R + \delta_1 = 0$:

$$0 = r + \delta_0 R + \delta_1,$$

$$\Rightarrow R = \frac{-(r + \delta_1)}{\delta_0}.$$

Since δ_0, δ_1, $r > 0$, we have $R = \frac{-(r+\delta_1)}{\delta_0} < 0$. But we are only interested in non-negative solutions. Hence this is not a biologically feasible solution.

Case 2 $T \neq 0$ *and* $B \neq 0$.

Solving for B in equation (4.7) we obtain

$$B = \frac{a_1 T^2}{d(c_2 + T^2)}. \tag{4.11}$$

Case 2.1 $E = 0$ *and* $R = 0$.

Under these assumptions, (4.6) reduces to

$$0 = a_0 T(1 - c_0 T).$$

Hence, $T = \frac{1}{c_0}$. *Substituting into (4.11),*

$$B = \frac{a_1(\frac{1}{c_0})^2}{d(c_2 + (\frac{1}{c_0})^2)} = \frac{a_1}{d(1 + c_2 c_0^2)}.$$

Hence, we have obtained the tumor escape solution: $T = 1/c_0$, $B = \frac{a_1}{d(1+c_2 c_0^2)}$,

$E = R = 0$.

Case 2.2 $E \neq 0$ *and* $R \neq 0$.

We will first obtain two equations describing E in terms of T. We then proceed by numerically obtaining solutions to this 2 equation system.

We begin by substituting (4.11) into (4.6) and solving for E.

$$0 = a_0 T(1 - c_0 T) - \delta_0 \frac{ET}{a + c_1(\frac{a_1 T^2}{d(c_2 + T^2)})},$$

$$\frac{\delta_0 E}{\frac{a_1 c_1 T^2 + d(c_2 + T^2)}{d(c_2 + T^2)}} = a_0(1 - c_0 T),$$

$$\frac{\delta_0 dE(c_2 + T^2)}{dc_2 + T^2(a_1 c_1 + d)} = a_0(1 - c_0 T),$$

$$E = \frac{a_0(1 - c_0 T)[dc_2 + T^2(a_1 c_1 + d)]}{\delta_0 d(c_2 + T^2)}. \tag{4.12}$$

We continue by substituting (4.11) into (4.8) and solving for E.

$$0 = \frac{fT}{1 + c_3 T(\frac{a_1 T^2}{d(c_2 + T^2)})} - r - \frac{\delta_0 r}{\delta_1} E - \delta_1,$$

$$\frac{\delta_0 r}{\delta_1} E = \frac{fT}{1 + c_3 T(\frac{a_1 T^2}{d(c_2 + T^2)})} - r - \delta_1,$$

$$E = \frac{\delta_1 fT}{r\delta_0 + \frac{c_3 \delta_0 r a_1 T^3}{d(c_2 + T^2)}} - \frac{\delta_1}{\delta_0} - \frac{\delta_1^2}{\delta_0 r},$$

$$E = \frac{\delta_1 fTd(c_2 + T^2)}{r\delta_0 d(c_2 + T^2) + c_3 \delta_0 r a_1 T^3} - \frac{\delta_1}{\delta_0} - \frac{\delta_1^2}{\delta_0 r}. \tag{4.13}$$

We are looking for E and T such that both (4.12) and (4.13) are satisfied. In Figure 4.6, we graph the function g(T) for the parameter values given by Table 4.1. This function is obtained by subtracting the RHS of (4.12) and (4.13) from each other and is defined as :

$$g(T) = \frac{a_0(1 - c_0 T)[dc_2 + T^2(a_1 c_1 + d)]}{\delta_0 d(c_2 + T^2)} - \frac{\delta_1 fTd(c_2 + T^2)}{r\delta_0 d(c_2 + T^2) + c_3 \delta_0 r a_1 T^3} - \frac{\delta_1}{\delta_0} - \frac{\delta_1^2}{\delta_0 r}.$$

$$\tag{4.14}$$
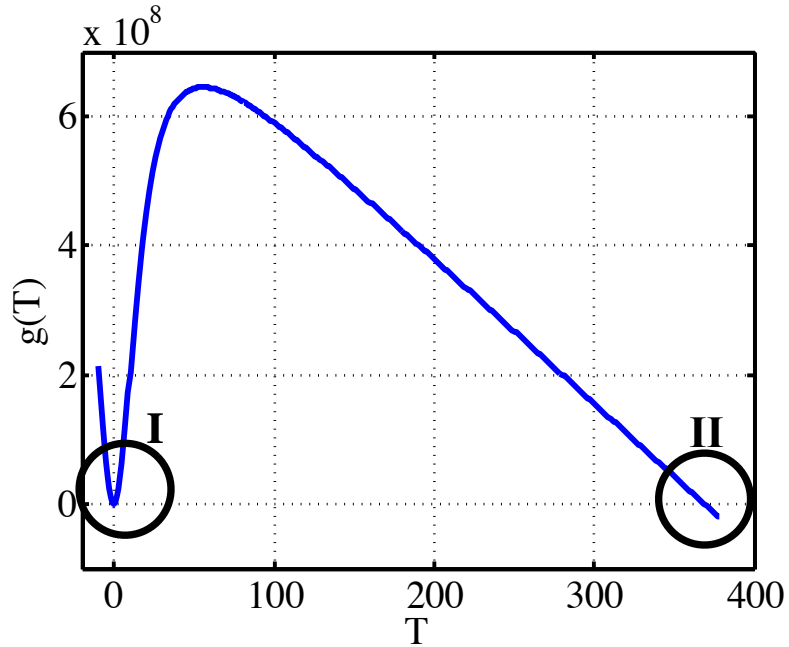
Figure 4.6: A graph of $g(T)$ (from (4.14)) for the relevant values of T. Visual inspection shows $g(T)$ has two regions containing possible zeros. These regions of interest are circled and labeled (I) and (II).

There are two areas of interest that possibly contain zeros. They are labeled (I) and (II) in Figure 4.6. Area (I) of Figure 4.6 is shown in Figure 4.7(a), and for the given parameters, (4.14) has no zeros in this region. Area (II) of Figure 4.6 is shown in Figure 4.7(b). Using bisection method, we numerically locate a zero at $T_0 = 368.87$. Substituting T_0 into (4.12) or (4.13), yields $E = -1.00052$. Again, we are only interested in steady states with non-negative values for all components. Hence, this is not a biologically feasible solution and does not need to be further considered.
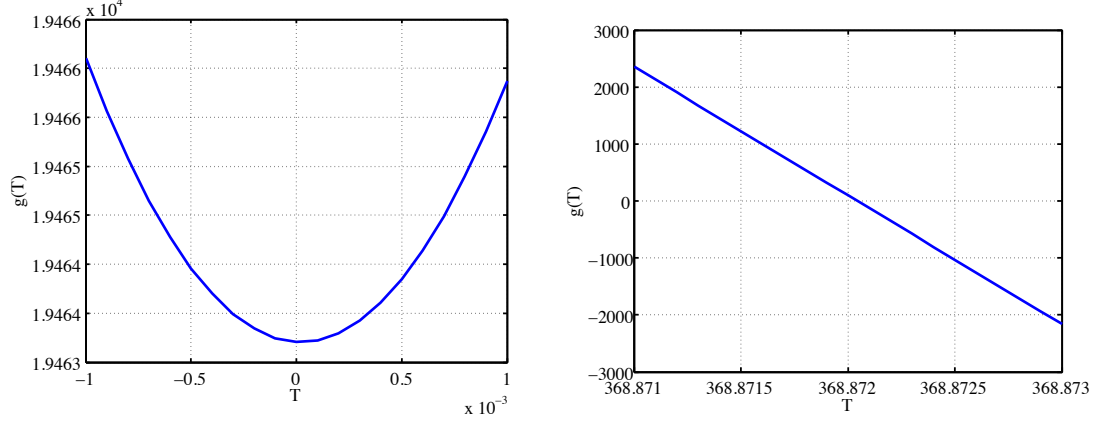
(a) A graph of $g(T)$ in region I of Figure 4.6. (b) A graph of $g(T)$ in region II of Figure 4.6.

Figure 4.7: $g(T)$ graphed in the regions of interest circled in Figure 4.6.

In order to analyze the stability of these equilibrium points, we consider the Jacobi matrix of $(4.1) - (4.4)$ with $V \equiv 0$. It is as follows:

$$
\begin{pmatrix}
a_0(1 - 2c_0 T) - \frac{\delta_0 E}{1+c_1 B} & \frac{\delta_0 c_1 ET}{(1+c_1 B)^2} & \frac{-\delta_0 T}{1+c_1 B} & 0 \\[2ex]
\frac{2Ta_1 c_2}{(c_2+T^2)^2} & -d & 0 & 0 \\[2ex]
\frac{fE}{(1+c_3 TB)^2} & \frac{-fc_3 ET^2}{(1+c_3 TB)^2} & \frac{fT}{1+c_3 TB} - r - \delta_0 R - \delta_1 & -\delta_0 E \\[2ex]
0 & 0 & r & -\delta_1
\end{pmatrix}
\tag{4.15}
$$

The steady state analysis of the system revealed two feasible (non-negative) steady states. Considering the eigenvalues of (4.15) when evaluated at these equilibria, the solution including maximum tumor capacity, $T = 1/c_0$, $B = \frac{a_1}{d(1+c_2 c_0^2)}$, $E = R = 0$, is stable while the all zero, $T = B = E = R = 0$, solution is unstable. This implies that even in the case of successful treatment, simulations will eventually lead to a non-zero tumor equilibrium. Hence, we consider treatment to be successful if the size of the tumor is reduced to less than the size of one cell or if the tumor is reduced to a "manageable" size for the duration of simulation.

89

As previously mentioned, all other steady states contain at least one negative component, implying that they are not feasible for the given biological system. This implies that there is no "small-tumor" equilibrium in which a tumor is maintained at a non-zero, non-lethal size by immune cells. In Figure 4.8, we present a phase portrait displaying the relation between tumor size and effector cells when combined treatment is simulated. Here we see that for tumors with high antigenicity, the tumor load is reduced to near zero for a period of time before the immune response is no longer able to control the tumor. For mildly antigenetic tumors, effector cells are only mildly stimulated by the presence of the tumor and cannot impose tumor shrinkage to manageable levels.
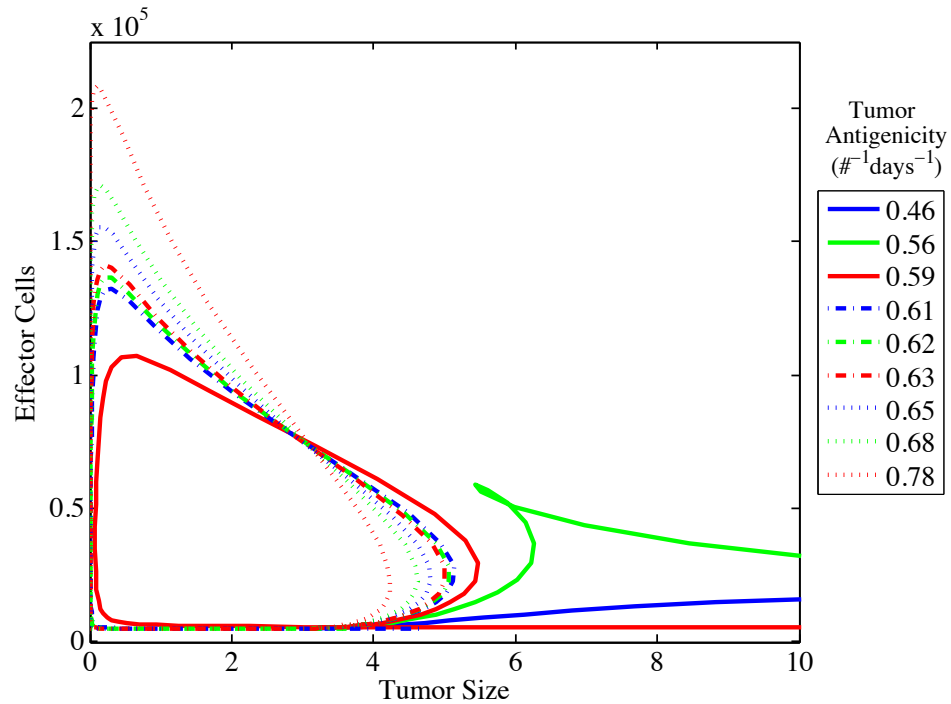
Figure 4.8: Effector T cell versus tumor size phase portrait when combined treatment is simulated with different levels of tumor antigenicity. Depending on the antigenicity, the tumor load is reduced to near zero for a period of time before the immune response is no longer able to control the tumor.

To determine the parameters to which the model is most sensitive, we performed a sensitivity analysis. This was done in a one-at-a-time fashion by varying each parameter over a range of values centered around a baseline value and observing the size of the tumor at the end of 30 simulated days. Figure 4.9 shows the results of this parameter sensitivity analysis with Figure 4.9(a) and Figure 4.9(b) displaying the results for the no treatment case and the combined treatment case, respectively. In the no treatment case, variations of parameters leads to very little changes in the final tumor size. This shows that, for a wide range of cases, a lack of treatment will lead to uncontrolled tumor growth. In the case of combined treatment, the system was found to be sensitive to a_1, the parameter quantifying the maximal production rate of TGF-β, c_2, the quantity describing the size at which a tumor begins to produce TGF-β, and f, the quantification of a tumor's antigenicity. The system is most sensitive to the parameter f which aligns with the results concerning the corresponding parameters in [29] and [62].
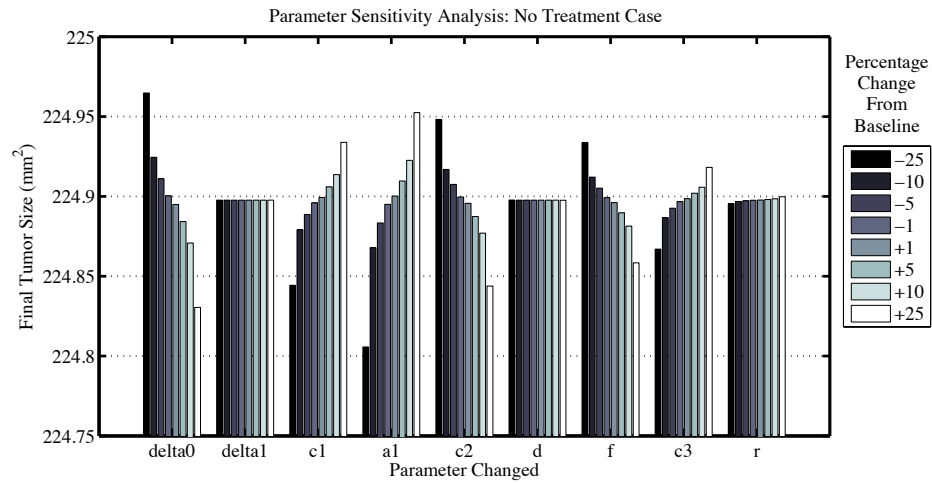
(a) No Treatment Sensitivity Analysis. Baseline values: $c_1 = 100$, $a_1 = 0.3$, $c_2 = 300$, $d = 7 \times 10^{-4}$, $f = 0.62$, $c_3 = 300$, $r = 0.01$
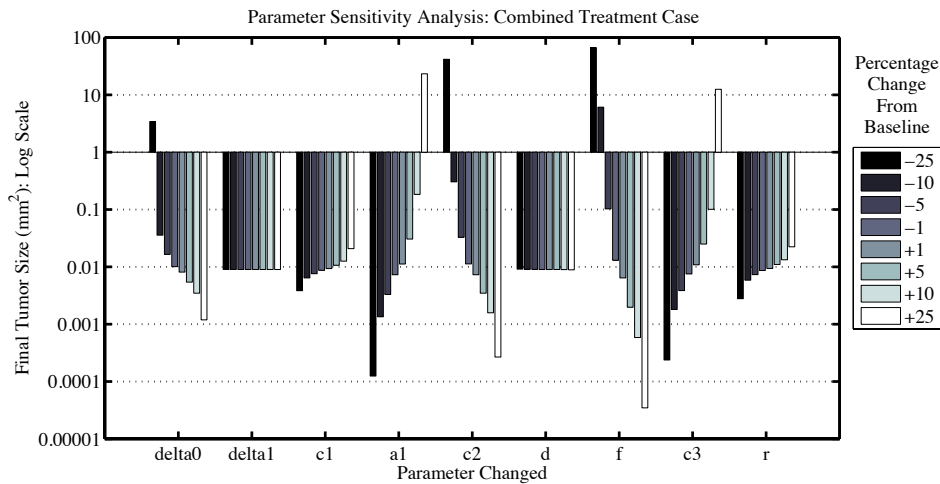
(b) Combined Treatment Sensitivity Analysis. Baseline values: $c_1 = 100$, $a_1 = 0.3$, $c_2 = 7 \times 10^3$, $d = 7 \times 10^{-4}$, $f = 0.62$, $c_3 = 300$, $r = 0.01$

Figure 4.9: Model sensitivity analysis. Done by varying each parameter over a range of values centered around a baseline value and observing the size of the tumor at the end of 30 simulated days. (a) No treatment case: variations of parameters leads to very little changes in the final tumor size. (b) Combined treatment: the system was found to be sensitive to a_1, the parameter quantifying the maximal production rate of TGF-β, c_2, the quantity describing the size at which a tumor begins to produce TGF-β, and f, the quantification of a tumor's antigenicity.

Due to the expression of the HPV E6 and E7 genes, the type of tumor considered for the model is considered to be reasonably antigenic. What happens if a less antigenic tumor is considered? This case is considered in Figure 4.10. Here, we reduce the value of the tumor antigenicity parameter, f. As previously mentioned, our sensitivity analysis suggests that the final tumor size is sensitive to this parameter. Figure 4.10 shows the results of reducing f from 0.62 by 10% to 0.56. In this case, there is a mild immune reaction, peaking around day 20 after tumor presentation. This immune response is capable of reducing the size of the tumor. However, the reduction of antigenicity causes the immune response to be unsustainable, leading to the eventual unbounded growth of the tumor.
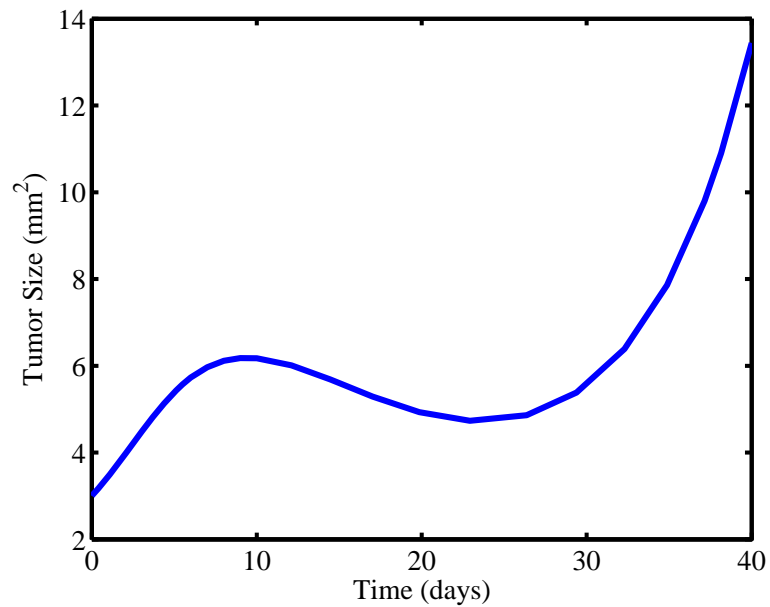
Figure 4.10: A simulated tumor growth for a mildly antigenic tumor ($f = 0.56$)

4.4 Discussion

The qualitative aspects of the simulations align with the data described in [106]. Obtaining precise quantitative matches with the data proved difficult as the data was presented as averages without error estimates or statistical measurements. However, the general characteristics of each of the four cases has been captured by the present model. For instance, in the case where both vaccine and TGF-β inhibitors were given, the model predicts that the tumor size will reach its peak on day 5 and tumor eradication will occur on day 21. The data suggests that these events occur respectively on days 15 and 27. Also, unlike the data presented by Terabe *et al.*, in which TGF-β inhibition lead to no significant delay in tumor growth, the model displays a slowed down (yet uncontrollable) tumor growth in the case of a TGF-β treatment. Modifying the model to better capture the timing of these events will be considered in future work. The choice of modeling the vaccine as an adoptive T cell transfer as opposed to a peptide vaccine could be one of the causes for the discrepancy in timing. In the model, T cells are immediately available to begin killing tumor cells, where as in the case of a peptide vaccine there would be a delay between the time of the vaccine and the time that newly recruited CTLs would be activated and available. This design choice contributes to the lack of need of delay differential equations and makes the model amendable to the study of questions regarding adoptive T cell transfer.

The means by which tumors evolve is nontrivial and all aspects of tumor treatment cannot be included in a single model. Our mathematical model highlights

just one possible way of combining tumor treatments to promote tumor eradication through an immune response. A number of biological experiments and mathematical models have highlighted the fact that immunotherapy alone is not always effective in eradicating a tumor [1, 22, 27, 33, 44, 62, 106]. Here we show how combined immunotherapy treatments might work through different mechanisms to promote tumor clearance. Simulations of model (4.1)–(4.5) show qualitative agreement with the data in [106]. In the case of administering either the vaccine or the TGF-β inhibitor, we see a temporary delay in tumor growth; but, this delay is not sustainable over time. The vaccine alone is not enough to eradicate the tumor, and though TGF-β is inhibited in the initial days of tumor presentation, the protein level recovers soon thereafter, regaining its immunosuppressive effects. Tumor eradication requires a combination of therapeutic approaches. Our results suggest that the vaccine allows for the development of a significant and long-term immune response that is minimally affected by the TGF-β that is present at later time points. The TGF-β inhibitor provides conditions that help the populations of immune cells to expand during the initial phases of tumor presentation. One very pertinent follow up question is: does one treatment amplify the other or do they act independently of each other? The data collected in [106] seems to support the notion that one treatment amplifies the other, but further study is required in order to reach a conclusive understanding.

The results of this work provide an initial analytical framework for studying immunotherapy via TGF-β inhibition in combination with vaccine treatment. Optimally, future studies should be conducted in combination with experiments. Control

of nonlinear processes will play a vital role in determining the effectiveness of these treatments and in obtaining a protocol for their administration.

Chapter 5

General Conclusions

Immune regulation is an essential component of the cell mediated immune response. Failure of regulatory control of the immune system can lead to a number of complications including autoimmune diseases and immune deficiency. Despite significant study of these topics, many immunoregulatory mechanisms are not well understood. In an effort to increase understanding of this topic, we use mathematical models to study the dynamics of immune regulation with a focus on the role of immune regulation in the primary immune response, immunodominance and tumor growth.

In chapters 2 and 3 we developed mathematical models of the primary immune response. We followed the hypothesis that regulatory T cells are an essential component in suppressing a normal immune response and included adaptive regulation as a key component of each of our models. We also highlighted the biological evidence regarding the ability of regulatory T cells to lose their regulatory capabilities and become immune promoting cells. In Chapter 2, we included the adaptive regulation and regulatory T cell switching mechanisms in an ODE model. We demonstrated that the model displays the expected expansion/contraction dynamics and conducted a study of the effects of Treg switching. Active suppression by regulatory T cells was shown to be a plausible mechanism of immune contraction. Negative

feedback provided by regulatory T cells was able to control the immune expansion and return the system to homeostasis. The regulatory T cell switching mechanism was shown to increase the robustness of the system, allowing for recovery from an unbalanced or even helper T cell deficient system.

A further exploration of these mechanisms was done in the context of a more detailed DDE model of the immune response in Chapter 3. Here, we demonstrated that when compared to previous mathematical models, our model shows increased robustness with respect to precursor T cell frequencies. Consistent with results found in Chapter 2, we identified a plausible range for the rate of Treg switching. This model is also used to study the effects of regulatory T cell switching on immunodominance. Treg switching was shown to affect immunodominance hierarchies in two ways. First, increasing the switching rate was shown to increase the magnitude of the immune response within a T cell clone hierarchy. Also, larger values of this rate were shown to increase the ability of weaker T cell clones to compensate for more dominant clones that were removed.

There are many avenues for further study within the topic of immune regulation. A spatial component can be added to the system by separating the lymph node from the infected tissue. Different cells have different functionalities depending on their environment and adding a spatial component would allow to account for these different functionalities. In such a compartmental model, one of the main questions to investigate would be whether regulatory cells are required at the infection site or if their presence in the lymph nodes is sufficient to robustly regulate the system.

All of the models presented here model the response to acute infections. These

models can be extended to study other occurrences such as chronic diseases or auto-immunity. It is unclear how memory cells influence the regulation of the immune system. Adding a memory T cell component is a key step in extending the applicability of our models from short-term, viral infections to chronic illnesses. Finally, regulatory T cells may play a key role in Human Immunodeficiency Virus (HIV) infections. HIV mainly affects activated helper T cells, leading to insufficient levels of these immune cells. Regulatory cells play a dual role in these infections. They reduce the number of activated helper T cells in the body, decreasing the number of possible targets for the virus. Yet this reduction also suppresses other mechanisms by which the immune system might fight the virus. Modeling the role that these cells play in HIV infections could lead to a better understanding of the nature of this disease.

In Chapter 4, we highlighted how immunotherapy might be used to overcome the effects of two immuno-regulatory agents exploited by cancer: regulatory T cells and the Transforming Growth Factor (TGF)-β protein. Our aim with this model was to understand part of the complexity of tumor immunology. Using the data presented in [106], we developed a mathematical model to gain insight into the cooperative interaction between anti-TGF-beta and vaccine treatments. Consistent with experiments of [106], our model demonstrated that monotherapy is not sufficient to eradicate a tumor and that tumor eradication requires the combination of these therapeutic approaches. Our results suggest that the vaccine provides a long-term immune response that is unaffected by the TGF-β present at later time points. The TGF-β inhibitor provides conditions that help the populations of immune cells

to expand during the initial phases of tumor presentation.

The alignment of our model with biological data suggests that this model can potentially be used in guiding future experiments that are aimed at studying immunotherapy as a treatment for cancer. The model can be potentially used to determine an optimal protocol for the administration of these immunotherapeutic approaches. To that end, optimal/suboptimal control of nonlinear processes will play a vital role in determining treatment protocols. A mathematical model of optimal control of multiple modes of tumor treatment is presented in [70]. Similar techniques can be used to consider combined anti-TGF-β and vaccine treatments. These theoretical protocols can then be followed by biological studies to determine their effectiveness.

Bibliography

[1] R. Akhurst and R. Derynck. TGF-β signaling in cancer – a double-edged sword. *Trends in Cell Biology*, 11(11):S44–S51, Nov. 2001.

[2] C. Althaus, V. Ganusov, and R. De Boer. Dynamics of CD8+ T cell responses during acute and chronic Lymphocytic Choriomeningitis Virus infection. *The Journal of Immunology*, 179(5):2944, 2007.

[3] I. J. Amanna and M. K. Slifka. Mechanisms that determine plasma cell lifespan and the duration of humoral immunity. *Immunological Reviews*, 236(1):125 – 138, 2010.

[4] R. Antia. Models of CD8+ responses: 1. What is the antigen-independent proliferation program. *Journal of Theoretical Biology*, 221(4):585–598, Apr. 2003.

[5] I. Apostolou and H. vonBoehmer. In vivo instruction of suppressor commitment in naïve t cells. *Journal of Experimental Medicine*, 199(10):1401–1408, 2004.

[6] A. Ay and D. N. Arnosti. Mathematical modeling of gene expression: a guide for the perplexed biologist. *Critical Reviews in Biochemistry and Molecular Biology*, 46(2):137–51, Apr. 2011.

[7] V. P. Badovinac, J. S. Haring, and J. T. Harty. Initial T cell receptor transgenic cell precursor frequency dictates critical aspects of the CD8(+) T cell response to infection. *Immunity*, 26(6):827–41, June 2007.

[8] C. Baecher-Allan, V. Viglietta, and D. A. Hafler. Human CD4+CD25+ regulatory T cells. *Seminars in Immunology*, 16(2):89 – 98, 2004.

[9] Baylor College of Medicine. Safety study of injections of autologous/allogeneic TGFBeta-resistant LMP2A-specific cytotoxic T lymphocytes (CTL). *Bethesda: National Library of Medicine*, 2006. Available from http://clinicaltrials.gov/ct/show/NCT00368082.

[10] Baylor College of Medicine. Her2 and TGFBeta in treatment of Her2 positive lung malignancy (HERCREEM). *Bethesda: National Library of Medicine*, 2009. Available from http://clinicaltrials.gov/ct/show/NCT00368082.

[11] Y. Belkaid, C. Piccirillo, S. Mendez, E. Shevach, and D. Sacks. CD4+CD25+ regulatory T cells control leishmania major persistence and immunity. *Nature*, 420(6915):502–507, 2002.

[12] N. Bellomo, E. De Angelis, and L. Preziosi. Multiscale modeling and mathematical problems related to tumor evolution and medical therapy. *Journal of Theoretical Medicine*, 5(2):111–136, 2003.

[13] E. Bettelli, T. Korn, M. Oukka, and V. K. Kuchroo. Induction and effector functions of T(H)17 cells. *Nature*, 453(7198):1051–7, June 2008.

[14] M. Beyer and J. L. Schultze. Regulatory T cells in cancer. *Blood*, 108(3):804–11, Aug. 2006.

[15] H. W. Blanch and D. S. Clark. *Biochemical engineering*. Marcel Dekker Inc., New York, 1997.

[16] J. N. Blattman, R. Antia, D. J. D. Sourdive, X. Wang, S. M. Kaech, K. Murali-Krishna, J. D. Altman, and R. Ahmed. Estimating the precursor frequency of naive antigen-specific CD8 T cells. *Journal of Experimental Medicine*, 195(5):657–64, Mar. 2002.

[17] J. N. Blattman and P. D. Greenberg. Cancer immunotherapy: a treatment for the masses. *Science*, 305(5681):200–5, July 2004.

[18] L. Brandt, T. Benfield, H. Mens, L. N. Clausen, T. L. Katzenstein, A. Fomsgaard, and I. Karlsson. Low level of regulatory T cells and maintenance of balance between regulatory T cells and TH17 cells in HIV-1-infected elite controllers. *Journal of Acquired Immune Deficiency Syndromes*, 57(2):101–108, 2011.

[19] F. M. Burnet. Immunological surveillance in neoplasia. *Immunological Reviews*, 7(1):3–25, 1971.

[20] H. Byrne and S. Gourley. The role of growth factors in avascular tumour growth. *Mathematical and Computer Modelling*, 26(4):35–55, Aug. 1997.

[21] R. Callard, A. J. George, and J. Stark. Cytokines, chaos, and complexity. *Immunity*, 11(5):507–513, Nov. 1999.

[22] A. Cappuccio, M. Elishmereni, and Z. Agur. Cancer immunotherapy by interleukin-21: potential treatment strategies evaluated in a mathematical model. *Cancer Research*, 66(14):7293–300, July 2006.

[23] F. Castiglione and B. Piccoli. Optimal control in a model of dendritic cell transfection cancer immunotherapy. *Bulletin of Mathematical Biology*, 68(2):255–74, Feb. 2006.

[24] A. Cerwenka and S. L. Swain. TGF-β1: immunosuppressant and viability factor for T lymphocytes. *Microbes and Infection*, 1(15):1291–6, Dec. 1999.

[25] W. Chen, W. Jin, N. Hardegen, K. Lei, L. Li, N. Marinos, G. McGrady, and S. Wahl. Conversion of peripheral CD4+CD25- naïve T cells to CD4+CD25+ regulatory T cells by TGF-β induction of transcription factor Foxp3. *Journal of Experimental Medicine*, 198(12):1875–1886, 2003.

[26] D. C. Clarke and X. Liu. Decoding the quantitative nature of TGF-beta/Smad signaling. *Trends in Cell Biology*, 18(9):430–42, Sept. 2008.

[27] G. Currie. Eighty years of immunotherapy: a review of immunological methods used for the treatment of human cancer. *British Journal of Cancer*, 26:141–153, 1972.

[28] L. G. de Pillis, W. Gu, and A. E. Radunskaya. Mixed immunotherapy and chemotherapy of tumors: Modeling, applications and biological interpretations. *Journal of Theoretical Biology*, 238(4):841–862, 2006.

[29] L. G. de Pillis, A. Radunskaya, and C. L. Wiseman. A validated mathematical model of cell-mediated immune response to tumor growth. *Cancer Research*, 65(17):7950–8, Sept. 2005.

[30] R. J. DeBoer, A. A. Freitas, and A. S. Perelson. Resource competition determines selection of B cell repertoires. *Journal of Theoretical Biology*, 212(3):333 – 343, 2001.

[31] R. J. DeBoer, D. Homann, and A. Perelson. Different dynamics of CD4+ and CD8+ T cell responses during and after acute lymphocytic choriomeningitis virus infection. *Journal of Immunology*, 171(8):3928 – 3935, Oct. 2003.

[32] C. Dejaco, C. Duftner, B. Grubeck-Loebenstein, and M. Schirmer. Imbalance of regulatory T cells in human autoimmune diseases. *Immunology*, 117(3):289–300, Mar. 2006.

[33] S. Dermime, A. Armstrong, R. E. Hawkins, and P. L. Stern. Cancer vaccines and immunotherapy. *British Medical Bulletin*, 62:149–62, Jan. 2002.

[34] R. Derynck, R. J. Akhurst, and A. Balmain. TGF-β signaling in tumor suppression and cancer progression. *Nature Genetics*, 29(2):117–29, Oct. 2001.

[35] O. Dickmann and H. J. A. *Mathematical epidemiology of infectious diseases: model building, analysis, and interpretation.* John Wiley & Sons, Inc., 2000.

[36] A. d'Onofrio. A general framework for modeling tumor-immune system competition and immunotherapy: Mathematical analysis and biomedical inferences. *Physica D: Nonlinear Phenomena*, 208(3-4):220 – 235, 2005.

[37] J. Duarte, S. Zelenay, M.-L. Bergman, A. Martins, and J. Demengeot. Natural Treg cells spontaneously differentiate into pathogenic helper cells in lymphopenic conditions. *European Journal of Immunology*, 39(4):948–55, Apr. 2009.

[38] R. Eftimie, J. Bramson, and D. Earn. Interactions between the immune system and cancer: A brief review of non-spatial mathematical models. *Bulletin of Mathematical Biology*, 73:2–32, 2011.

[39] N. J. Eungdamrong and R. Iyengar. Modeling cell signaling networks. *Biology of the Cell*, 96(5):355–62, June 2004.

[40] A. Farrell, E. Hutchinsin, and B. Marte. Nature milestones in cancer. *Nature*, 573(April):2281–2287, 2006.

[41] Z. Fehérvári and S. Sakaguchi. Control of Foxp3+ CD25+CD4+ regulatory cell activation and function by dendritic cells. *International Immunology*, 16(12):1769–1780, 2004.

[42] J. E. Ferrell. Self-perpetuating states in signal transduction: positive feedback, double-negative feedback and bistability. *Current Opinion in Cell Biology*, 14(2):140–148, Apr. 2002.

[43] M. A. Fishman and A. S. Perelson. Th1/Th2 differentiation and cross-regulation. *Bulletin of Mathematical Biology*, 61(3):403–36, May 1999.

[44] R. A. Flavell, S. Sanjabi, S. H. Wrzesinski, and P. Lixon-Limon. The polarization of immune cells in the tumour environment by TGFβ. *Nature Reviews Immunology*, 10(8):554–567, 2010.

[45] F. Ghiringhelli, N. Larmonier, E. Schmitt, A. Parcellier, D. Cathelin, C. Garrido, B. Chauffert, E. Solary, B. Bonnotte, and F. Martin. CD4+CD25+ regulatory Tcells suppress tumor immunity but are sensitive to cyclophosphamide which allows immunotherapy of established tumors to be curative. *European Journal of Immunology*, 34(2):336–344, 2004.

[46] N. J. Guido, X. Wang, D. Adalsteinsson, D. McMillen, J. Hasty, C. R. Cantor, T. C. Elston, and J. J. Collins. A bottom-up approach to gene regulation. *Nature*, 439(7078):856–60, Feb. 2006.

[47] D. M. Hamby. A review of techniques for parameter sensitivity analysis of environmental models. *Environmental Monitoring and Assessment*, 32(2):135–154, Sept. 1994.

[48] D. Hanahan and R. A. Weinberg. The hallmarks of cancer. *Cell*, 100(1):57–70, 2000.

[49] D. Hanahan and R. A. Weinberg. Hallmarks of cancer: The next generation. *Cell*, 144(5):646–674, Mar. 2011.

[50] H. Harringon. *Mathematical models of cellular decisions: investigating immune response and apoptosis*. PhD dissertation, Imperial College London, October 2010.

[51] H. A. Harrington, K. L. Ho, S. Ghosh, and K. C. Tung. Construction and analysis of a modular model of caspase activation in apoptosis. *Theoretical Biology & Medical Modelling*, 5:26, Jan. 2008.

[52] A. Hoare, D. G. Regan, and D. P. Wilson. Sampling and sensitivity analyses tools (SaSAT) for computational modelling. *Theoretical Biology & Medical Modelling*, 5:4, Jan. 2008.

[53] T. Hong, J. Xing, L. Li, and J. J. Tyson. A mathematical model for the reciprocal differentiation of T helper 17 cells and induced regulatory T cells. *PLoS Computational Biology*, 7(7):e1002122, July 2011.

[54] H. A. Huehn, J. Homing to suppress: Address codes for treg migration. *Trends in Immunology*, 26(12):632–636, 2005.

[55] J. Huehn, J. K. Polansky, and A. Hamann. Epigenetic control of FOXP3 expression: the key to a stable regulatory T-cell lineage? *Nature reviews. Immunology*, 9(2):83–9, Feb. 2009.

[56] B. Joshi, X. Wang, S. Banerjee, H. Tian, A. Matzavinos, and M. A. J. Chaplain. On immunotherapies and cancer vaccination protocols: a mathematical modelling approach. *Journal of Theoretical Biology*, 259(4):820–7, Aug. 2009.

[57] S. M. Kaech and R. Ahmed. Memory CD8+ T cell differentiation: initial antigen encounter triggers a developmental program in naïve cells. *Nature Immunology*, 2(5):415–22, May 2001.

[58] P. Kim, P. Lee, and D. Levy. Emergent group dynamics governed by regulatory cells produce a robust primary t cell response. *Bulletin of Mathematical Biology*, 72:611–644, 2010.

[59] P. Kim, P. Lee, and D. Levy. Basic principles in modeling adaptive regulation and immunodominance. In A. Friedman, E. Kashdan, U. Ledzewicz, and H. Schättler, editors, *Mathematical models and methods in biomedicine*. Springer, 2012.

[60] P. S. Kim, P. P. Lee, and D. Levy. Modeling regulation mechanisms in the immune system. *Journal of Theoretical Biology*, 246(1):33–69, May 2007.

[61] P. S. Kim, P. P. Lee, and D. Levy. A theory of immunodominance and adaptive regulation. *Bulletin of Mathematical Biology*, 73(7):1645–65, July 2011.

[62] D. Kirschner, T. Jackson, and J. Arciero. A mathematical model of tumor-immune evasion and siRNA treatment. *Discrete and Continuous Dynamical Systems - Series B*, 4(1):39–58, Nov. 2003.

[63] D. Kirschner and J. C. Panetta. Modeling immunotherapy of the tumor-immune interaction. *Journal of Mathematical Biology*, 37(3):235–52, Sept. 1998.

[64] D. Kirschner and A. V. Tsygvintsev. On the global dynamics of a model for tumor immunotherapy. *Mathematical Biosciences and Engineering*, 6(3):573–83, July 2009.

[65] L. Klein, K. Khazaie, and H. vonBoehmer. In vivo dynamics of antigen-specific regulatory T cells not predicted from behavior in vitro. *Proceedings of the National Academy of Sciences of the United States of America*, 100(15):8886–8891, 2003.

[66] Y. Kogan, U. Forys, O. Shukron, and N. Kronik. Cellular immunotherapy for high grade gliomas: Mathematical analysis deriving efficacious infusion rates based on patient requirements. *SIAM Journal on Applied Mathematics*, 70(6):1953–1976, 2010.

[67] M. Kolev. A mathematical model for single cell cancer immune system dynamics. *Mathematical and Computer Modelling*, 41:1083–1095, 2005.

[68] K. Kretschmer, I. Apostolou, D. Hawiger, K. Khazaie, M. Nussenzweig, and H. vonBoehmer. Inducing and expanding regulatory T cell populations by foreign antigen. *Nature Immunology*, 6(12):1219–1227, 2005.

[69] V. Kuznetsov, I. Makalkin, M. Taylor, and A. Perelson. Nonlinear dynamics of immunogenic tumors: Parameter estimation and global bifurcation analysis. *Bulletin of Mathematical Biology*, 56(2):295–321, 1994.

[70] U. Ledzewicz, H. Maurer, and H. Schaettler. Optimal and suboptimal protocols for a mathematical model for tumor anti-angiogenesis in combination with chemotherapy. *Mathematical Biosciences and Engineering*, 8(2):307–323, 2011.

[71] D. Llopiz, J. Dotor, N. Casares, J. Bezunartea, N. Daz-Valds, M. Ruiz, F. Aranda, P. Berraondo, J. Prieto, J. J. Lasarte, F. Borrs-Cuesta, and P. Sarobe. Peptide inhibitors of transforming growth factor-β enhance the efficacy of antitumor immunotherapy. *International Journal of Cancer*, 125(11):2614–2623, 2009.

[72] G. Marcais. *Genome assembly techniques*. PhD dissertation, University of Maryland, 2011.

[73] G. Marchuk. *Mathematical modelling of immune response in infectious diseases*. Kluwer Academic Publishers, Netherlands, 1997.

[74] D. Marquardt. An algorithm for least-squares estimation of nonlinear parameters. *Journal of the Society for Industrial and Applied Mathematics*, 11(2):431–441, 1963.

[75] R. Mercado, S. Vijh, S. E. Allen, K. Kerksiek, I. M. Pilip, and E. G. Pamer. Early programming of T cell populations responding to bacterial infection. *Journal of Immunology*, 165(12):6833–9, Dec. 2000.

[76] S. Michelson and J. Leith. Autocrine and paracrine growth factors in tumor growth: a mathematical model. *Bulletin of Mathematical Biology*, 53(4):639–56, Jan. 1991.

[77] M. Miyara, Y. Yoshioka, A. Kitoh, T. Shima, K. Wing, A. Niwa, C. Parizot, C. Taflin, T. Heike, D. Valeyre, A. Mathian, T. Nakahata, T. Yamaguchi, T. Nomura, M. Ono, Z. Amoura, G. Gorochov, and S. Sakaguchi. Functional delineation and differentiation dynamics of human CD4+ T cells expressing the FoxP3 transcription factor. *Immunity*, 30(6):899–911, June 2009.

[78] S. S. Miyara, M. Natural regulatory T cells: mechanisms of suppression. *Trends in Molecular Medicine*, 13(3):108–116, 2007.

[79] K. Murphy, P. Travers, and M. Walport. *Immunobiology*. Garland Science, New York, 2008.

[80] B. Novak, Z. Pataki, A. Ciliberto, and J. J. Tyson. Mathematical model of the cell division cycle of fission yeast. *Chaos*, 11(1):277–286, Mar. 2001.

[81] M. Nowak. Immune responses against multiple epitopes: a theory for immunodominance and antigenic variation. *Seminars in Virology*, 7(1):83–92, Feb. 1996.

[82] G. Oldenhove, N. Bouladoux, E. a. Wohlfert, J. a. Hall, D. Chou, L. Dos Santos, S. O'Brien, R. Blank, E. Lamb, S. Natarajan, R. Kastenmayer, C. Hunter, M. E. Grigg, and Y. Belkaid. Decrease of Foxp3+ Treg cell number and acquisition of effector cell phenotype during lethal infection. *Immunity*, 31(5):772–86, Dec. 2009.

[83] F. Paillard. Immunosuppression mediated by tumor cells: a challenge for immunotherapeutic approaches. *Human Gene Therapy*, 11(5):657–8, Mar. 2000.

[84] E. S. Razvi, Z. Jiang, B. a. Woda, and R. M. Welsh. Lymphocyte apoptosis during the silencing of the immune response to acute viral infections in normal, lpr, and Bcl-2-transgenic mice. *The American Journal of Pathology*, 147(1):79–91, July 1995.

[85] S. L. Reiner. Decision making during the conception and career of CD4+ T cells. *Nature Reviews Immunology*, 9(2):81–2, Feb. 2009.

[86] M. Reiss. TGF-β and cancer. *Microbes and Infection*, 1(15):1327–1347, Dec. 1999.

[87] T. Renno, A. Attinger, S. Locatelli, T. Bakker, S. Vacheron, and H. R. MacDonald. Cutting edge: apoptosis of superantigen-activated T cells occurs preferentially after a discrete number of cell divisions in vivo. *Journal of Immunology*, 162(11):6312–5, June 1999.

[88] A. Ribas, L. H. Butterfield, J. a. Glaspy, and J. S. Economou. Current developments in cancer vaccines and cellular immunotherapy. *Journal of Clinical Oncology*, 21(12):2415–32, June 2003.

[89] B. Ribba, T. Colin, and S. Schnell. A multiscale mathematical model of cancer, and its use in analyzing irradiation therapies. *Theoretical Biology & Medical Modelling*, 3:7, Jan. 2006.

[90] S. A. Rosenberg. Progress in human tumour immunology and immunotherapy. *Nature*, 411(6835):380–4, May 2001.

[91] S. A. Rosenberg, J. C. Yang, and N. P. Restifo. Cancer immunotherapy: moving beyond current vaccines. *Nature Medicine*, 10(9):909–15, Sept. 2004.

[92] Y. P. Rubtsov, R. E. Niec, S. Josefowicz, L. Li, J. Darce, D. Mathis, C. Benoist, and a. Y. Rudensky. Stability of the regulatory T cell lineage in vivo. *Science*, 329(5999):1667–1671, Sept. 2010.

[93] R. Ruddon. *Cancer biology, Fourth edition*. Oxford University Press, 2007.

[94] S. Sakaguchi. Conditional stability of T cells. *Nature*, 468:41–42, 2010.

[95] S. Sakaguchi, M. Miyara, C. M. Costantino, and D. A. Hafler. FOXP3+ regulatory T cells in the human immune system. *Nature Reviews Immunology*, 10(7):490–500, June 2010.

[96] S. Sakaguchi, T. Yamaguchi, T. Nomura, and M. Ono. Regulatory T cells and immune tolerance. *Cell*, 133(5):775–87, May 2008.

[97] B. Sather, P. Treuting, N. Perdue, M. Miazgowicz, J. Fontenot, A. Rudensky, and D. Campbell. Altering the distribution of Foxp3+ regulatory T cells results in tissue-specific inflammatory disease. *Journal of Experimental Medicine*, 204(6):1335–1347, 2007.

[98] L. F. Shampine, I. Gladwell, and S. Thompson. *Solving ODEs with Matlab*. Cambridge University Press, 2003.

[99] M. Shapiro-Shelef and K. Calame. Regulation of plasma-cell development. *Nature Reviews Immunology*, 5(3):230–242, 2005.

[100] E. Shevach. From vanilla to 28 flavors: multiple varieties of T regulatory cells. *Immunity*, 25(2):195–201, 2006. cited By (since 1996) 280.

[101] N. Smith, P. Mulquiney, and M. Nash. Mathematical modelling of the heart: cell to organ. *Chaos, Solitons & Fractals*, 13:1613–1621, 2002.

[102] H. Souza-e-Silva, W. Savino, R. a. Feijóo, and A. T. R. Vasconcelos. A cellular automata-based mathematical model for thymocyte development. *PloS One*, 4(12):e8233, Jan. 2009.

[103] M. B. Sporn. TGF-β: 20 years and counting. *Microbes and Infection*, 1(15):1251–1253, Dec. 1999.

[104] L. S. Taams, M. Vukmanovic-Stejic, J. Smith, P. J. Dunne, J. M. Fletcher, F. J. Plunkett, S. B. Ebeling, G. Lombardi, M. H. Rustin, J. W. J. Bijlsma, F. P. J. G. Lafeber, M. Salmon, and A. N. Akbar. Antigen-specific T cell suppression by human CD4+CD25+ regulatory T cells. *European Journal of Immunology*, 32(6):1621–30, June 2002.

[105] Q. Tang, J. Y. Adams, A. J. Tooley, M. Bi, B. T. Fife, P. Serra, P. Santamaria, R. M. Locksley, M. F. Krummel, and J. A. Bluestone. Visualizing regulatory T cell control of autoimmune responses in nonobese diabetic mice. *Nature Immunology*, 7(1):83–92, Jan. 2006.

[106] M. Terabe, E. Ambrosino, S. Takaku, J. J. O'Konek, D. Venzon, S. Lonning, J. P. McPherson, and J. A. Berzofsky. Synergistic enhancement of CD8+ T cell-mediated tumor vaccine efficacy by an antitransforming growth factor-β monoclonal antibody. *Clinical Cancer Research*, 15(21):6560–9, 2009.

[107] M. Tsuji, N. Komatsu, S. Kawamoto, K. Suzuki, O. Kanagawa, T. Honjo, S. Hori, and S. Fagarasan. Preferential generation of follicular B helper T cells from Foxp3+ T cells in gut Peyer's patches. *Science*, 323(5920):1488–92, Mar. 2009.

[108] M. J. van Stipdonk, G. Hardenberg, M. S. Bijker, E. E. Lemmens, N. M. Droin, D. R. Green, and S. P. Schoenberger. Dynamic programming of CD8+ T lymphocyte responses. *Nature Immunology*, 4(4):361–5, Apr. 2003.

[109] M. J. van Stipdonk, E. E. Lemmens, and S. P. Schoenberger. Naïve CTLs require a single brief period of antigenic stimulation for clonal expansion and differentiation. *Nature Immunology*, 2(5):423–9, May 2001.

[110] H. von Boehmer. Mechanisms of suppression by suppressor T cells. *Nature Immunology*, 6(4):338–344, 2005.

[111] Y. Y. Wan and R. A. Flavell. Regulatory T-cell functions are subverted and converted owing to attenuated Foxp3 expression. *Nature*, 445(7129):766–70, Feb. 2007.

[112] S. E. Wang, P. Hinow, N. Bryce, A. M. Weaver, L. Estrada, C. L. Arteaga, and G. F. Webb. A mathematical model quantifies proliferation and motility effects of TGF-β on cancer cells. *Computational and Mathematical Methods in Medicine*, 10(1):71–83, 2009.

[113] S. Wilson and D. Levy. A mathematical model of the enhancement of tumor vaccine efficacy by immunotherapy. *Bulletin of Mathematical Biology*, (accepted).

[114] S. N. Wilson, P. Lee, and D. Levy. A mathematical model of the primary t cell response with contraction governed by adaptive regulatory T cells. In K. E. Herold, W. E. Bentley, and J. Vossoughi, editors, *Proc. IFMBE*, volume 32, pages 209–212. Springer, 2010.

[115] K. Wing, Y. Onishi, P. Prieto-Martin, T. Yamaguchi, M. Miyara, Z. Fehervari, T. Nomura, and S. Sakaguchi. CTLA-4 control over Foxp3+ regulatory T cell function. *Science*, 322(5899):271–275, Oct. 2008.

[116] D. Wodarz and A. R. Thomsen. Effect of the CTL proliferation program on virus dynamics. *International Immunology*, 17(9):1269–1276, September 2005.

[117] T. Yamaguchi, K. Hirota, K. Nagahama, K. Ohkawa, T. Takahashi, T. Nomura, and S. Sakaguchi. Control of immune responses by antigen-specific regulatory T cells expressing the folate receptor. *Immunity*, 27(1):145–159, 2007.

[118] S. Yamazaki, T. Iyoda, K. Tarbell, K. Olson, K. Velinzon, K. Inaba, and R. Steinman. Direct expansion of functional CD25+ CD4+ regulatory T cells by antigen-processing dendritic cells. *Journal of Experimental Medicine*, 198(2):235–247, 2003.

[119] A. Yates, C. Bergmann, J. L. Van Hemmen, J. Stark, and R. Callard. Cytokine-modulated regulation of helper T cell populations. *Journal of Theoretical Biology*, 206(4):539–60, Oct. 2000.

[120] X. Zhou, S. L. Bailey-Bucktrout, L. T. Jeker, C. Penaranda, M. Martínez-Llordella, M. Ashby, M. Nakayama, W. Rosenthal, and J. A. Bluestone. Instability of the transcription factor Foxp3 leads to the generation of pathogenic memory T cells in vivo. *Nature Immunology*, 10(9):1000–7, Sept. 2009.